

**Natural and anthropogenic drivers of
Australian temperature extremes, simulated
over the last millennium**

by

Tanya Lippmann

Supervisors:

Dr. Lisa Alexander

and

Dr. Steven Phipps

November 2012

Declaration

I hereby declare that this thesis contains no material which has been accepted for a degree or diploma by the University or any other institution, except by way of background information and duly acknowledged in the thesis; that, to the best of my knowledge and belief, this thesis contains no material previously published or written by another person, except where due acknowledgment is made in the text of the thesis; and that this thesis does not contain any material which infringes copyright.

Signed: _____

Tanya Lippmann

Acknowledgements

Software used for this project and thesis included Mk3L Climate System Model (Mk3L), Ferret (www.ferret.noaa.gov/Ferret) and Matlab (www.mathworks.com.au). All code used for data manipulation, and data analysis was stored in Git repositories, using github.com. The LATEX code for this document was stored in a similar fashion. The model runs were conducted on the University of New South Wales (UNSW) Mathematics Departments Tensor computing cluster. All data was stored on the Climate Change Research Centre (CCRC)s shared data facilities and the National Computational Infrastructure (NCI) Sun Constellation VAYU cluster. Financial support through an honours scholarship was received from the Australian Research Council (ARC) Centre of Excellence for Climate System Science. I would like to thank my supervisors Steven Phipps and Lisa Alexander for their supervision and guidance.

Abstract

Research has built extensive knowledge of most climate drivers and a detailed timeline of the climatic changes that have occurred over the past millennium. However, many cause and effect relationships are not yet robustly understood. Assessment of mean temperature can dangerously mask extremes that have a profound impact on human society and the natural environment. The daily temporal resolution required to assess climate extremes has confined much previous research to the observational record. This research seeks to understand the relationship between climate drivers (internal and external, natural and anthropogenic) and temperature extremes in Australia over the last 1000 years.

Natural variability is a strong driver of temperature extremes in Australia. Cloudiness relates to the variability of all extreme indices. El Niño Southern Oscillation is a strong contributor to the variability of hottest days in Australia. Cloudiness, the Indian Ocean Dipole and the Interdecadal Pacific Oscillation drive the variability of coldest days; which exhibits almost no signal from external forcings.

Solar irradiance and volcanism act as a dynamic duo driving temperature extremes. Across Australia volcanic eruptions cause large and abrupt cooling; although this cooling is not necessarily proportional to the size of eruption. Solar forcing is found to have little influence on temperature extremes but enhances (or reduces) and temporally extends (or shortens) the impact of volcanic eruptions on temperature extremes.

The anthropogenic signal dominates during the industrial period, where T_{max} indices exhibit larger trends and are generally heavily influenced by external forcings. T_{min} indices on the other hand, either maintain complex relationships with external climate drivers or are primarily forced by the internal climate variability.

The findings of this study indicate that the relative influences of external forcings and natural variability differ for each index. Because of the influence of natural variability and the potential for external forcings to amplify and dampen each other, the response to a specific external forcing is not necessarily proportional to the signal.

Contents

Declaration	ii
Acknowledgements	iii
Abstract	iv
1 Introduction	2
1.1 Climate extremes	3
1.2 Climate of the last millennium	5
1.3 Australian climate	5
1.4 Drivers of temperature extremes	6
1.4.1 External drivers	7
1.4.2 Internal variability	8
1.4.3 Anthropogenic forcings	9
1.5 Aims	9
2 Methodology	11
2.1 Extreme indices	11
2.2 Description of the model, Mk3L	12

2.3	Forcings and experiments	14
2.4	Trends and statistical significance	16
3	Model-data comparison	18
3.1	Observational data sets	18
3.2	Results of comparison	20
3.2.1	Model minus observations	20
3.2.2	Trends	22
3.2.3	Confidence intervals	23
3.2.4	Variability	23
3.3	Summary of model evaluation	25
4	Results	26
4.1	Internal variability	26
4.1.1	Hottest days	28
4.1.2	Hottest nights	29
4.1.3	Coldest days	30
4.1.4	Coldest nights	31
4.1.5	Summary of internal variability	31
4.2	External drivers	32
4.2.1	Volcanic eruptions	32
4.2.2	Summary of volcanic forcing	36
4.2.3	Solar Irradiance	36
4.2.4	Summary of solar forcings	37

4.3	Dynamic duo; volcanic and solar forcings	38
4.3.1	Summary of dynamic duo	42
4.4	Anthropogenic drivers	42
4.4.1	Summary of anthropogenic forcing	45
4.5	Variability of temperature extremes over the last millennium	46
4.5.1	Inter-decadal variability	46
4.5.2	Spatial variability of extremes over Australia	50
4.6	Summary of results	52
5	Discussion	53
5.1	External Drivers of temperature extremes	53
5.1.1	Volcanic eruptions	53
5.1.2	Solar Irradiance	55
5.1.3	Dynamic duo volcanic and solar forcings	55
5.1.4	Anthropogenic Forcing	56
5.2	Variability of Australian temperature extremes	58
5.3	Other limitations of this study	61
6	Conclusions and future work	62
6.1	Conclusions	62
6.2	Future work	63

List of Figures

2.1	Forcings on the climate system	15
3.1	Model minus observations difference plots	21
3.2	Time series over observational period	24
4.1	Correlations with dynamical drivers	27
4.2	OGV and OGSV anomalies relative to the pre-industrial mean	33
4.3	OGV minus OG composite time series of volcanic eruptions	34
4.4	Spatial distribution of volcanic composite	35
4.5	OGS and OG anomalies relative to the pre-industrial period	37
4.6	OGS minus OG during the Maunder Minimum	38
4.7	OGSV minus OG time series composite of volcanic eruptions	40
4.8	OGSV minus OG composite of three largest volcanoes	41
4.9	O temperature extreme anomalies relative to pre-industrial period	43
4.10	Time series and trends over the 1900's	44
4.11	T_{max} anomalies	47
4.12	T_{min} anomalies	48
4.13	Year-to-year variability	51

List of Tables

2.1	Summary of indices	11
2.2	Summary of forcings	16
2.3	Summary of volcanoes	16
3.1	Observational data sets	19
3.2	Decadal trends	22
3.3	Variability of observations and the model	23
4.1	Correlations between extremes and dynamical modes - DJF	29
4.2	Correlations between extremes and dynamical modes - JJA	29
4.3	Statistical significance of anthropogenic GHG	44
4.4	Variability of extreme indices	47

Chapter 1

Introduction

There is growing evidence that the current change in climate will be accompanied by a significant increase in both the frequency and impact of some extreme weather and climate events (Seneviratne *et al.*, 2012). In a changing climate, frequency, duration and severity of climate extremes are likely to have profound and significant impacts on communities and ecosystems; both human society and the natural environment (e.g. Karl & Easterling, 1999; Alexander & Arblaster, 2009; Min *et al.*, 2011). Independent of any changes or trends of climate extremes themselves, society is becoming more vulnerable to climate extremes and the cost of mitigating against and adapting to climate extremes is becoming more expensive (Adger *et al.*, 2003; Tompkins & Adger, 2004).

Mean global temperature has often been used as the index to describe climate change (Stott & Kettleborough, 2002; Simmons, 2004; Smith *et al.*, 2009). However, this metric is not necessarily relevant at a local or seasonal scale. An alternative is to look at extreme weather phenomena, which can have significant impacts at local and regional scales on both society and ecosystems. However, these can be difficult to define and have long return periods, adding uncertainty to assessment (Zhang *et al.*, 2011). This study

uses temperature extreme indices that are able to capture moderately extreme climate phenomena that occur frequently enough to statistically identify changes (Frich *et al.*, 2002; Alexander & Arblaster, 2009).

Australia is a continent containing many climatic regimes from tropical, to desert, to temperate. It is a land of extremes where rivers “run dry or ten feet high” (Friedel *et al.*, 1990). Australia is influenced by many large scale phenomena, generating a naturally very variable climate. The Australian continent provides an opportunity to assess many climates, modes of variability and their relationships with external forcings.

The extent of daily observational data required for the study of extremes has confined previous research to the latter half of the twentieth century. The observational period is a very small window and may not be an accurate representation of longer term behaviour. Analysis of a much longer record is required to identify the influences of external and anthropogenic forcings, internal climate variability on temperature extremes (Mann, 2007; Hegerl *et al.*, 2007). Past climate forms the basis of future climate and similarly, understanding past climate forms the basis of understanding future climate, presenting the following key question:

How and why have Australian daily temperature extremes changed over the past millennium?

1.1 Climate extremes

Extremes at regional scales may exhibit different and often much larger amplitudes than at global scales, and thus the effect of extremes on natural environments and human societies may be misjudged (Easterling *et al.*, 2000; Briffa & Osborn, 2002). Australia’s

already extreme climate may be either more susceptible or more adaptable to changing climate extremes relative to other regions. Understanding this relationship is of benefit to Australia as a country, and may provide an indication of how other regions that experience similar climates will adapt when faced with similar climate stressors.

Previous assessments of climate extremes have used observational datasets (Frich *et al.*, 2002; Alexander *et al.*, 2006). Research has now expanded to include natural proxy records (e.g. Luterbacher *et al.*, 2004) and climate models (e.g. Tebaldi *et al.*, 2006). Observational data most closely resembles the real world but records are temporally and spatially limited (Solomon *et al.*, 2007a). Proxy records extend farther back in time but have limited accuracy and coarse spatial & temporal resolution (Mann *et al.*, 2008). Climate models avoid these issues, however, each model is accompanied by its own limitations and therefore, must be well evaluated against observations or proxies (Kiktev *et al.*, 2007; Nicholls & Alexander, 2007; Jones *et al.*, 2009). The use of climate models to assess climate extremes is still relatively novel and little research has been undertaken to understand how non-anthropogenic climate forcings drive climate extremes.

For this study, I have only assessed temperature extremes, as past studies have shown these to be well simulated by Global Climate Models (GCMs). Comparisons using GCMs participating in the Intergovernmental Panel on Climate Change (IPCC) diagnostic exercise for the Fourth Assessment Report (AR4) and Coupled Model Intercomparison Project (CMIP), as well as others GCMs have shown that models are less successful at reproducing precipitation-related extreme indices (Alexander & Arblaster, 2009; Kharin *et al.*, 2007; Kiktev *et al.*, 2007; Perkins *et al.*, 2007). For this reason precipitation related extreme indices are not assessed in this study. To assess the ability of Mk3L to reproduce the temperature extreme indices used here, the model is evaluated against several observational data sets.

1.2 Climate of the last millennium

The long term global climate trend over the past millennium is best described as a modest and irregular cooling from approximately 1000 to 1900, followed by an abrupt twentieth century warming (Bradley *et al.*, 2003). A warm period early in the millennium known as the Medieval Climate Anomaly (MCA; \sim 950–1250; Lamb, 1965); a cool period from the 14th to 17th centuries known as the Little Ice Age (LIA; \sim 1400–1700; Matthes, 1939); and rapid warming during the twentieth century characterise the climate over this period. The existence of the MCA, LIA and recent twentieth century warming are supported by multiple studies. Nonetheless, few conclusions can be made regarding the relative influence of natural and unnatural forcings and, internal and external climate drivers on temperature. Furthermore, the availability of data has restricted a great deal of this research to the Northern Hemisphere (NH). Limited availability of proxy data and regional inconsistencies have led to disagreement as to whether either the MCA or LIA were global or hemispheric epochs (Hughes & Diaz, 1994; Jones *et al.*, 2001; Mann *et al.*, 2009; Fernández-Donado *et al.*, 2012). See Diaz *et al.* (2011) for review of the literature. Both climate anomalies are thought to have largely been driven by a combination of solar and volcanic forcings (e.g. Crowley, 2000; Rind, 2002; Hegerl *et al.*, 2007). This study uses GCM, Mk3L (Phipps *et al.*, 2011) to assess the past thousand years of extreme temperature over Australia.

1.3 Australian climate

The Australian climate is spatially variable and spanning from the tropics to temperate zones, this gives rise to nonuniform climate changes. The Australian climate has experienced large changes over the twentieth century and even larger changes are projected for

the twenty-first century (Allen *et al.*, 2000; Stott & Kettleborough, 2002; Smith *et al.*, 2009). The Australian continent is subject to several atmospheric and oceanic modes of variability that have a trans-hemispheric influence; for example, El Niño-Southern Oscillation (ENSO; e.g. Jones & Trewin, 2000; Wang & Hendon, 2007), Interdecadal Pacific Oscillation (IPO; e.g. Kenyon & Hegerl, 2008), Southern Annular Mode (SAM; e.g. Hendon *et al.*, 2007), and Indian Ocean Dipole (IOD; e.g. Hendon, 2003; Risbey *et al.*, 2009). During El Niño, Eastern Australia experiences warmer, drier conditions and this is reversed during La Niña. The IOD is a coupled ocean and atmosphere phenomenon that affects the climate and particularly the rainfall of Australia. The Australian continent provides an opportunity to assess many climates, modes of variability and their relationships with external forcings.

During the twentieth century, temperature and precipitation extremes have changed significantly across Australia (Plummer *et al.*, 1999; Collins & Della-Marta, 2000; Alexander *et al.*, 2007). The frequency and intensity of most extreme rainfall and temperature events are rising faster than means (Alexander *et al.*, 2007). Since 1950, southern and eastern Australia have become drier, whilst the north-western two-thirds of Australia have seen an increase in summer monsoon rainfall (Smith, 2004; Hendon *et al.*, 2007). Higher temperatures and decreased rainfall have resulted in increased severity of drought (Nicholls & Alexander, 2007).

1.4 Drivers of temperature extremes

The high temporal resolution required to assess temperature extremes restricts most previous work to the observational period, with a focus on anthropogenic greenhouse gases (GHG) as the dominant driver. This means little attention has been paid to understanding how other drivers, and even internal variability, influence temperature extremes. The

climate of the last millennium has been characterised by volcanic eruptions, solar irradiance fluctuations, changing concentrations of GHG, and modes of internal variability (Steinhilber *et al.*, 2012). Therefore, these forcings are a focus of this study.

1.4.1 External drivers

There is evidence that solar irradiance, volcanism, GHG (Lean *et al.* 1995; Crowley & Kim, 1996; Hegerl *et al.* 2003) and to a lesser extent changes in the Earth's orbit (Jones & Mann 2004) have forced climate over the past millennium. Forcings are defined as external perturbations to the climate system and are referred to as external forcings in the context of this study; for example, solar irradiance, volcanism and changes to the Earth's orbit. However, modes of internal variability within the ocean-atmosphere system also perturb the Australian climate and are therefore referred to as 'internal' forcing within the context of this study.

Volcanic eruptions eject ash and sulphuric compounds into the atmosphere that give rise to the formation of aerosols, increasing the optical depth of the atmosphere. Volcanic eruptions generally result in net cooling of surface temperatures (Robock, 2000). The distribution of volcanic aerosols occurs by atmospheric circulation leading to regional (mainly dependent on latitude) and temporal (mainly seasonal) differences. The volcanic reconstruction of Crowley *et al.* (2008) finds the largest eruption of the millennium occurred in 1258 (unknown location) and exhibited an estimated radiative forcing of -11.2 Wm^{-2} . The volcanic eruption of Mount Tambora, Indonesia is the second largest of the period (-7.2 Wm^{-2}) and occurred in 1815. The third largest volcanic eruption (Kuwae, Vanuatu) happened in 1456 (-5.5 Wm^{-2}).

Solar variability is the change in the amount of radiation emitted by the sun and has

the potential to force the Earth’s climate by varying solar input and directly altering the planetary energy budget. An anomalous period of high solar radiation occurred early in the millennium (often associated with the MCA) and anomalous periods of low solar radiation, the grand minima, during the LIA (Steinhilber *et al.*, 2012). The extent to which solar variations impact climate is a topic of much controversy and a great number of papers have presented evidence of its dominance (e.g. Servonnat *et al.*, 2010; Foukal *et al.*, 2006), and lack of statistical significance (e.g. Crowley, 2000; Mann & Cane, 2005).

Variation in the Earth’s orbit and concentrations of naturally occurring GHG have also occurred over the pre-industrial period of the last millennium, but these are thought to have played less dominant roles as climate drivers (Servonnat *et al.*, 2010). In this study, the pre-industrial period is considered to be anything prior to 1850.

The most recent climate anomaly is evident in the instrumental record and is thus considerably less debated in the literature. Almost the entire globe has experienced temperatures significantly warmer in the late twentieth century than earlier in the millennium. These have been attributed to increasing anthropogenic greenhouse gases (Bauer, 2003; Zorita, 2005; Osborn & Briffa, 2006).

1.4.2 Internal variability

Modes of climate variability; for example, ENSO, the North Atlantic Oscillation (NAO) and the Pacific Decadal Oscillation (PDO), require accurate representation in model simulations if they are to be able to robustly reproduce climate extremes (Shindell *et al.*, 2003; Jones & Mann, 2004; Scaife *et al.*, 2008; Kenyon & Hegerl, 2008). ENSO has an important influence on climate extremes around the world (Kenyon & Hegerl, 2008; Alexander *et al.*, 2009) and is the dominant mode of interannual climate variability

on Earth (McPhaden *et al.*, 2006; Li *et al.*, 2011). The behaviour of ENSO is complex, chaotic, and highly variable. Because of low-frequency variability, 500+ years need to be examined to capture the baseline of ENSO and its characteristics (Wittenberg, 2009).

1.4.3 Anthropogenic forcings

Natural changes in GHG concentrations have occurred over the past millennium but more recently, anthropogenic changes to GHG concentrations have become a dominant driver of global climate variability (MacFarling Meure *et al.*, 2006). It is evident from temperature proxy records that the late twentieth century warming is large and unprecedented relative to recent millennia (Hegerl *et al.*, 2007; Mann, 2007). An anthropogenic signal must be included in model simulations to reproduce observed changes in climate extremes (Crowley, 2000; Kiktev *et al.*, 2007; Alexander & Arblaster, 2009). These trends have generated increasing concern that climate extremes are changing in frequency and intensity because of anthropogenic increases in GHG.

1.5 Aims

The observational period provides a small window into climatic behaviour, and therefore may not be an accurate representation of the longer term climate system. Assessing the influence of forcings on climate extremes over the last millennium allows for identification of relationships between climate extremes and other variables in the climate system that may be anomalous over the observational period. There is also consensus that modern warming can be at least partially attributed to anthropogenic forcings. The influence of particular forcings on other climatic variables can be difficult to identify as instrumental data coincides with this anomalous period. Climate models such as Mk3L

allow assessment of a wide range of relationships as model simulations encompass long-term physical mechanisms and processes within the climate system. Understanding all the processes that have driven temperature extremes over the last millennium is beyond the scope of this thesis. However, this thesis offers a stepping stone to further understand these relationships.

Chapter 2

Methodology

2.1 Extreme indices

Table 2.1 specifies the four temperature extreme indices used in this study. These indices are only a selection of the twenty seven climate extremes indices defined by ETCCDI (Karl & Easterling, 1999; Zhang *et al.*, 2011)¹. The indices used in this study were chosen to assess changes in intensity of the following absolute events: *hottest days*, *coldest days*, *hottest nights* and *coldest nights* of a year.

Index	Definition	Description
TXx	Annual maximum value of daily maximum temperature	Hottest days
TNx	Annual maximum value of daily minimum temperature	Hottest nights
TXn	Annual minimum value of daily maximum temperature	Coldest days
TNn	Annual minimum value of daily minimum temperature	Coldest nights

Table 2.1: A selection of the temperature extreme indices recommended by the ETCCDI to be used in this study.

¹CCI/CLIVAR/JCOMM Expert Team on Climate Change Detection and Indices (ETCCDI); <http://ccma/seos.uvic.ca/ETCCDI>

2.2 Description of the model, Mk3L

This study uses version 1.2 of the CSIRO climate system model, Mk3L. This is a reduced resolution GCM model configured for millennial scale climate simulations and palaeoclimate research (Phipps *et al.*, 2011). Mk3L is a fully coupled general circulation model and includes components describing the atmosphere, ocean, sea ice and land surface. Phipps *et al.* (2011) describe and evaluate the model, and Phipps *et al.* (2012b) discuss its response to external forcings. Mk3L was designed to combine a realistic climatology with computational efficiency, ideal for palaeoclimate research. The atmosphere, land and sea-ice components are reduced resolution versions of those used by the CSIRO Mk3 coupled model (Gordon *et al.*, 2002). Mk3 contributed towards CMIP3 (Meehl *et al.*, 2007) and the IPCC AR4 (Solomon *et al.*, 2007b). Another version, Mk3.6.0 is a contributing model to CMIP5 and the IPCC Fifth Assessment Report (AR5; Collier *et al.*, 2011). Phipps *et al.* (2012a) study the role of external forcings in driving the global climate over the past 1500 years through assessment of Mk3L against proxy records using several forced simulations that are used in this study.

The atmospheric component of Mk3L has 18 vertical levels; with horizontal resolutions of 5.6° longitude by 3.2° latitude for the atmosphere, sea ice and land surface models (Phipps *et al.*, 2011). The oceanic component has a resolution of 2.8° longitude by 1.6° latitude and 21 vertical levels. The model features both a cumulus convection scheme and a prognostic stratiform cloud scheme. The radiation scheme simulates full annual and diurnal cycles of longwave and shortwave radiation (Phipps *et al.*, 2011).

Mk3L produces a realistic simulation of the modern climate (Phipps *et al.*, 2011). The control state of the model is able to maintain a high degree of stability, producing only a weak cooling on millennial timescales. Mk3L does not include biophysical components such as dynamic vegetation or representation of the global carbon cycle. The

leading modes of internal climate variability are reasonably well represented across the globe. This means that the spatial and temporal variability associated with ENSO is well represented. However, the model simulates a slightly extended ENSO cycle relative to observations (Sanotoso *et al.*, 2011). The model successfully simulates the magnitude and spatial patterns of modern twentieth century warming, consistent with observations.

Mk3l does not include an aerosol scheme or atmospheric chemistry, restricting the realism of the representation of solar and volcanic forcings and anthropogenic aerosols (Phipps *et al.*, 2012b). In simulations of the last millennium, the model underestimates the relative warmth associated with the MCA and fails to reproduce the La Nina-like pattern of temperature changes apparent over the Pacific Basin. However, it is able to simulate an appropriate transition from the MCA to the LIA. Relative to reconstructions, the model overestimates cooling in response to the volcanic eruption of 1258. In the Southern Hemisphere, the model's response to solar and volcanic forcings is more robust relative to global analysis and the palaeoclimate reconstruction of Mann *et al.* (2009), (Phipps *et al.*, 2012a). Overall, the model is able to successfully reproduce the global climate of the last millennium (Phipps *et al.*, 2012b) and responds realistically to climate forcings, particularly in the SH (Phipps *et al.*, 2012a,b).

The spatial resolution of Mk3L

Mk3L's spatial resolution renders it very computationally efficient, enabling multiple forced simulations to be run over millennia. Whilst there are state-of-the-art high resolution coupled models that simulate the observed climate better than Mk3L, at the present time these are not practical for multi-millennial simulations or large ensembles, due to computational limitations. Mk3L balances computational efficiency, a relatively strong climatology and numerical efficiency.

Perkins *et al.* (2007) found coarse resolution models smoothed orography, limiting the ability of models to simulate minimum temperature (T_{min}) indices. Encouragingly, CSIRO Mk3 was ranked second best of all models; based on its ability to reproduce minimum & maximum temperatures and precipitation. A review of the literature does not suggest that the resolution of Mk3L will hinder the model’s ability to reproduce temperature extremes. Indeed, Alexander & Arblaster (2009) indicated that model resolution was not critical for the simulation of temperature extremes. Mk3L’s ability to reproduce temperature extremes is evaluated by comparison with observational daily data sets (Chapter 3).

2.3 Forcings and experiments

To appreciate the influence of an external forcing, it is necessary to disentangle the multiple nonlinear feedbacks that can amplify or diminish the climate forcing as well as change the nature and consistency of the response. To do this, multiple model simulations were run over the past millennium with various combinations of external forcings. Model simulations were forced with combinations of the following anthropogenic and natural forcings: changes in the Earth’s orbital parameters (Berger, 1978), concentrations of greenhouse gases (MacFarling Meure *et al.*, 2006), solar irradiance (Steinhilber *et al.*, 2009), and volcanic eruptions (Crowley *et al.*, 2008) each with reasonably well constrained boundary conditions (e.g. Schmidt *et al.*, 2012). The model was initialised in 1 CE and then run to equilibrium under permanent pre-industrial boundary conditions. Orbital, greenhouse gases, solar, and volcanic forcings were progressively included and therefore, simulations O, OG, OGS, OGV and OGSV were initialised from the control simulation at varying years within the first millennium. In total, five model simulations were run, although only the last 1000 years of each will be assessed here. The control

simulation is not used for assessment. Phipps *et al.* (2012b) assesses the model’s response to external forcings. Variations in each climate forcing over the past 1000 years are shown in Figure 2.1.

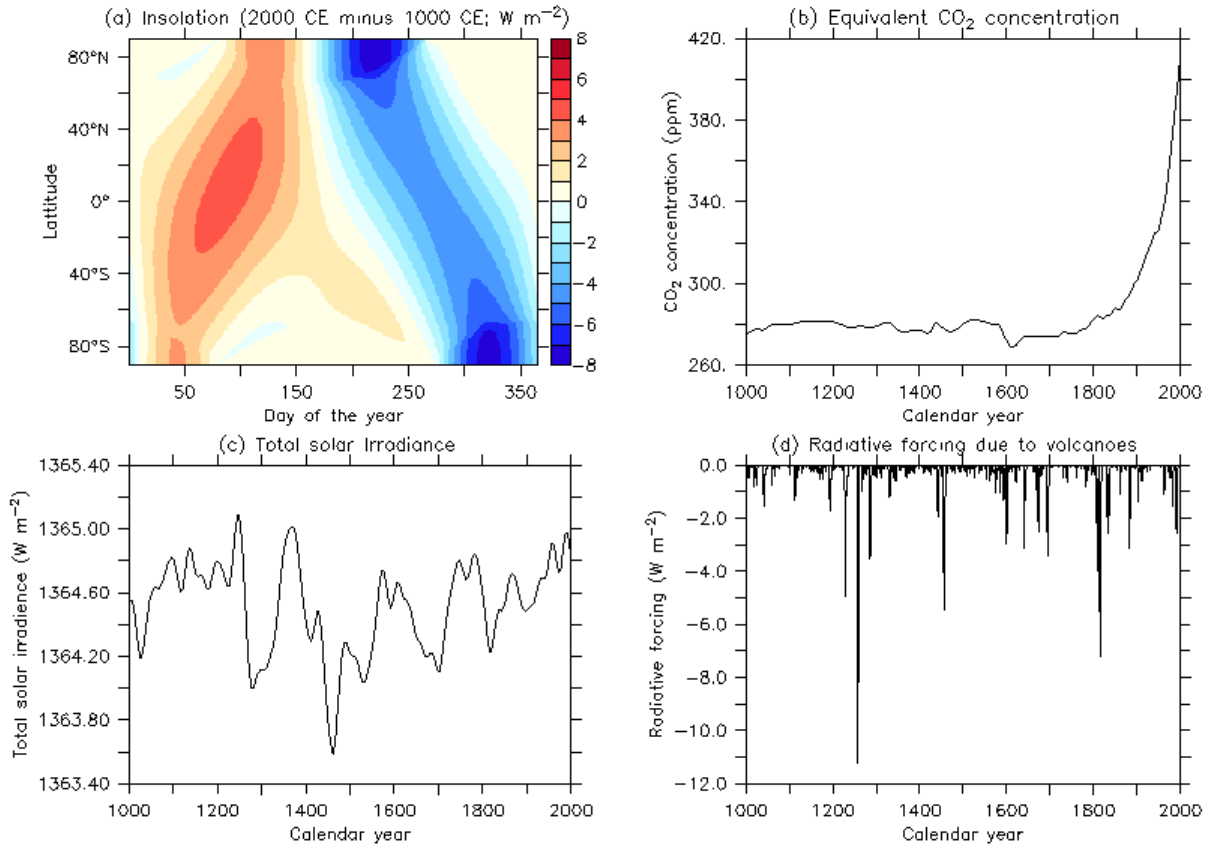


Figure 2.1: The forcings on the climate system between 1000 CE and 2000 CE: (a) Changes in the distribution of insolation due to changes in the Earth’s orbital geometry (Wm^{-2} ; Berger, 1978), (b) the equivalent CO_2 concentration (ppm; MacFarling Meure *et al.*, 2006), (c) total solar irradiance (Wm^{-2} ; Steinhilber *et al.*, 2009), (d) the radiative forcing due to volcanic eruptions (Wm^{-2} ; Crowley *et al.*, 2008).

The following combinations of forcings are applied to Mk3L as summarised in Table 2.2: orbital only (O); orbital and greenhouse gases (OG); orbital, greenhouse gases and solar irradiation (OGS); orbital, greenhouse gases and volcanic activity (OGV); and orbital, greenhouse gases, solar irradiation, and volcanic activity (OGSV). The role of each forcing

is able to be distinguished by comparison between each simulation. Extreme indices (Table 2.1) were calculated for all model simulations.

Abbreviation	Forcing(s)
O	Orbital
OG	Orbital, greenhouse gases
OGS	Orbital, greenhouse gases, solar irradiance
OGV	Orbital, greenhouse gases, volcanic aerosols
OGSV	Orbital, greenhouse gases, solar irradiance, volcanic aerosols

Table 2.2: A summary of forcings applied to climate model simulations. Their values can be found in Figure 2.1.

The three largest volcanic eruptions that have occurred within the last thousand years are listed in Table 2.3. These eruptions were chosen to assess the influence of volcanism on temperature extremes. In order of magnitude they are and will be referred to in the text as: 1258, Tambora and Kuwae. To assess the influence of changes in solar irradiation, the Maunder Minimum (1645–1715) was chosen as the only anomalously cool period that does not coincide with large volcanic eruptions.

Location	Year	Effective Radiative Forcing
Unknown	1258	-11.2 Wm ⁻²
Mount Tambora, Indonesia	1815	-7.2 Wm ⁻²
Kuwae, Vanuatu	1456	-5.5 Wm ⁻²

Table 2.3: The three largest volcanic eruptions that have occurred over the last millennium. Radiative forcing due to volcanism are estimates based on ice core reconstructions (Figure 2.1d; Crowley *et al.*, 2008).

2.4 Trends and statistical significance

Trends are calculated using ordinary least squares (OLS) regression. OLS is sensitive to series outliers and does not account for autocorrelation in time series residuals, which may be present in extremes. However, it has been shown that these indices are not

highly correlated in time and that OLS trends are robust for extreme temperature indices (Alexander & Arblaster, 2009).

A students t-test is used to test the null hypothesis that there is no statistically significant difference between (i) forced and unforced simulations (ii) the preindustrial mean and a forced climatological event or anomalous period. A 95% confidence interval is used to test significance.

Chapter 3

Model-data comparison

3.1 Observational data sets

The observational data sets used for model evaluation are outlined in Table 3.1. All available datasets containing adequate observations within Australia were used for comparison (Table 3.1). All seven datasets have varying spatial coverage across Australia and have used different interpolation techniques to produce gridded fields. The methodology and level of quality control varies amongst datasets. Using a broad spread of datasets to perform model evaluation increases the comprehensiveness of the model assessment and confidence in the conclusions with respect to dataset uncertainties.

The Global Historical Climatology Network-Daily Dataset (GHCN-Daily; Durre *et al.*, 2010) provide the source of data for GHCN AUS (Vogel, 2012), HadGHCND (Caesar *et al.*, 2006) and GHCNDEX (Donat *et al.*, 2012b). These three datasets were created and are managed independently of GHCN-Daily. HadGHCND, for example, calculates indices after gridding unlike GHCN AUS and GHCNDEX. HadEX1 (Alexander *et al.*,

Data set	Quality controlled?	Time period compared	Reference
GHCNDEX	No	1957-2000	Donat <i>et al.</i> (2012b)
GHCN AUS	No	1957-2000	Vogel (2012)
HQ AUS	Yes	1957-2000	Haylock & Nicholls (2000); Trewin (2001); Vogel (2012)
HadGHCND	Some	1957-2000	Caesar <i>et al.</i> (2006)
HadEX1	Yes	1957-2000	Alexander <i>et al.</i> (2006)
HadEX2	Yes	1911-2000	Donat <i>et al.</i> (2012a)
AWAP	Some	1911-2000	Jones & Wang (2009); Vogel (2012)

Table 3.1: Summary of observational data sets used for model evaluation.

2006) and HadEX2 (Donat *et al.*, 2012a) are quality controlled datasets each compiled from a number of smaller dataset initiatives, GHCND-Daily and ETCCDI. The HQ dataset, gridded by Vogel (2012) and originally created by Haylock & Nicholls (2000); Trewin (2001), is quality controlled for inhomogeneities. The HQ AUS, AWAP and GHCN AUS datasets used here were each regridded onto a 3° by 3° grid by Vogel (2012).

Of the datasets used, most contain data for Australian stations that were adjusted for inhomogeneities after 1956 (Trewin, 2001). For this reason it was decided that 1957 would be a reasonable start date to begin model comparison. However, HadEX2 records extend to 1901 and AWAP records extend back to 1911. Therefore, where appropriate, model comparisons for AWAP and HadEX2 datasets start from 1911. The model simulations end in 2000, and therefore this was chosen as the end date for all comparisons.

Comparisons between observations and the model were performed over Australia only. These comparisons uses all forcings, i.e. simulation OGSV. Assessments based on Australian averages, such as time series and trend calculations, only use information containing grid boxes common to all datasets. It follows that limited observational spatial coverage can easily become a source of uncertainty (Donat & Alexander, 2012) when eval-

uating model performance. Using all available datasets and hence all available spatial data, maximises common spatial area, reduces uncertainty and increases confidence in Australian averaged calculations. Each dataset is based on a varying number of weather stations, has varying regional coverage, and is gridded at differing resolutions. Therefore, each dataset was interpolated onto the model's grid (5.6° by 3.2°) using weighted average interpolation.

Reanalysis data sets could potentially be used to aid model evaluation. However, the assimilation methods and varying station networks over time means they lack consistency relative to observational datasets, limiting their usefulness in this regard (Bengtsson *et al.*, 2004; Simmons, 2004; Brands *et al.*, 2012). Considering these factors and the availability of observational data sets over Australia, reanalyses were not used to aid model evaluation in this study.

3.2 Results of comparison

3.2.1 Model minus observations

Difference plots (model minus observations) are assessed to determine how well the model captures the spatial variations and magnitude of temperature extremes (Figure 3.1). Comparisons using AWAP and HadEX2 were performed over the period 1911-2000, whilst comparisons with other datasets are restricted to 1957-2000 (Section 3.1).

The model is generally too cool for *coldest days* and too warm for *hottest nights* (Figure 3.1). The model overestimates (underestimates) the intensity of *hottest days* in north eastern (south western) Australia. The model also produces a cooler central Australia and warmer coastal Australia for the *coldest nights* index. For the most part, differ-

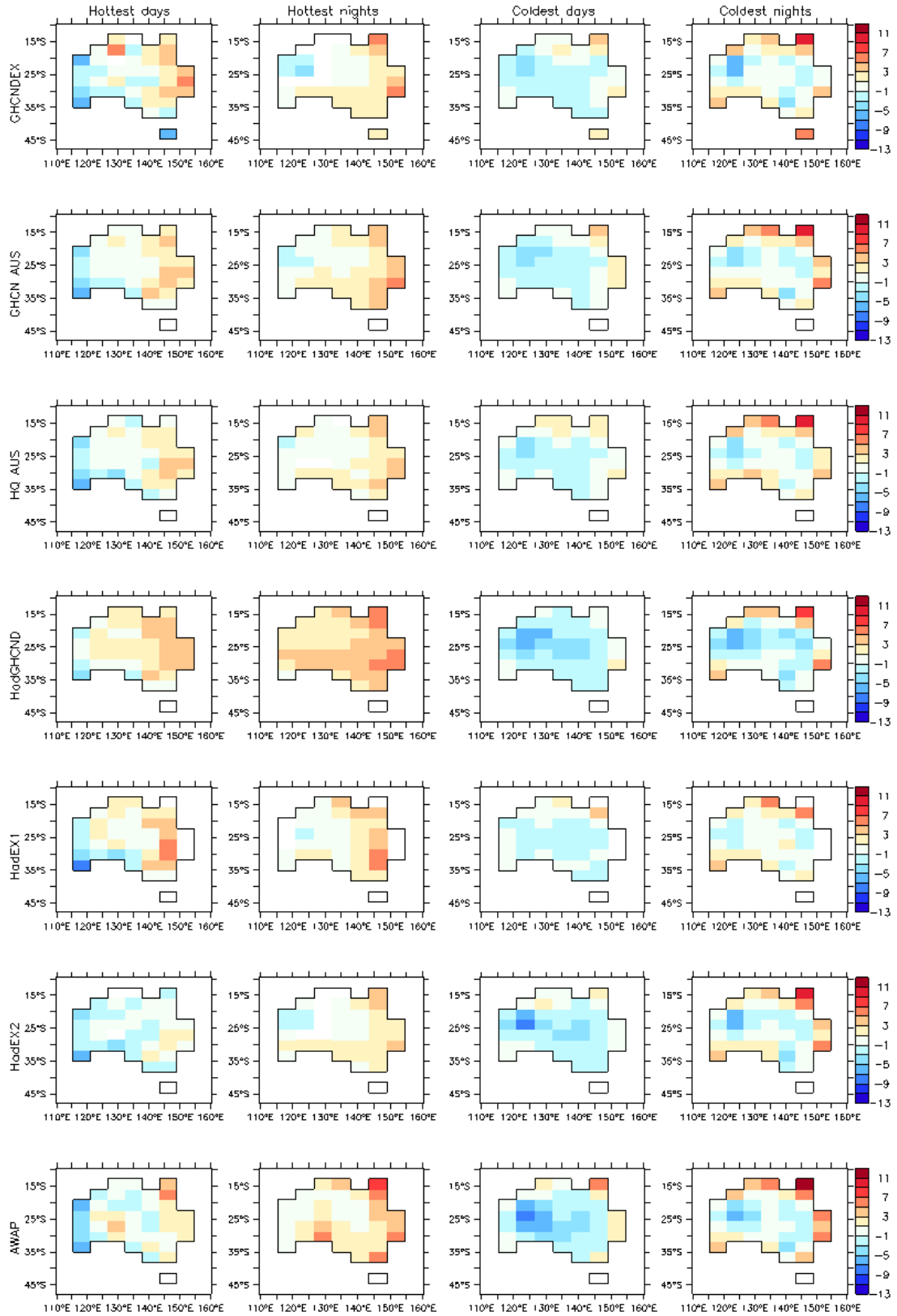


Figure 3.1: Model minus observed temperature extremes. AWAP and HadEX2 are compared over the period 1911-2000 (averaged) whereas, all other datasets are compared over the period 1957-2000 (averaged). Units are $^{\circ}\text{C}$.

ences between the model and observation are within $\pm 5^\circ\text{C}$ and the spatial patterns of differences for each index are broadly similar irrespective of which dataset is used for comparison (Figure 3.1).

3.2.2 Trends

Australian averaged time series and trend calculations are generated over the period 1957-2000 (Figure 3.2 and Table 3.2, respectively). In order that comparable analysis can be performed, only grid boxes where observed data exist are used. Confidence intervals are calculated to assess the uncertainty in trend calculations.

Dataset	TX _x	TN _x	TX _n	TN _n
GHCNDEX	+0.02(-0.13/0.17)	+0.18(0.02/0.34)	+0.24(0.03/0.44)	+0.43(0.26/0.60)
GHCN AUS	+0.02(-0.13/0.17)	+0.14(0.03/0.36)	+0.27(0.08/0.47)	+0.23(0.08/0.38)
HQ AUS	+0.02(-0.14/0.18)	+0.19(0.03/0.36)	+0.28(0.08/0.49)	+0.35(0.20/0.50)
HadGHCND	0.00(-0.16/0.16)	+0.23(0.07/0.38)	+0.27(0.07/0.47)	+0.34(0.18/0.50)
HadEX1	+0.06(-0.12/0.24)	+0.21(0.05/0.38)	+0.30(0.09/0.50)	+0.44(0.27/0.60)
HadEX2	+0.05(-0.11/0.21)	+0.21(0.04/0.38)	+0.28(0.07/0.50)	+0.32(0.16/0.48)
AWAP	+0.04(-0.12/0.20)	+0.24(0.06/0.41)	+0.24(0.02/0.46)	+0.25(0.08/0.41)
Mk3L (model)	+0.16(0.07/0.26)	+0.15(0.03/0.27)	+0.20(-0.16/0.57)	+0.24(0.12/0.37)

Table 3.2: Observed and modelled linear trends calculated over 1957-2000 for each index (see Table 2.1 for index definitions). Trends are calculated using grid boxes containing observations common to all datasets and averaged across Australia. Boldface indicates trends that are significant at the 5% level. 5 and 95% confidence intervals are shown in brackets. Units are $^\circ\text{C}$ per decade.

The trends for each index are broadly similar irrespective of the dataset used for comparison. Relative to observations, the model successfully reproduces trends of the same sign for all indices (Table 3.2). Furthermore, all datasets and the model produce trends of the same order of magnitude for three indices; *hottest nights*, *coldest days* and *coldest*

nights trends. The model reproduces *hottest and coldest nights* particularly well as these indices fall within the breadth of observations. The model underestimates the trend in *coldest days* and overestimates the trend in *hottest days*. However, the spread between observational trends is less for *coldest and hottest days*, relative to other indices.

3.2.3 Confidence intervals

Confidence intervals (Table 3.2) for the model do not overlap with zero and are narrower than that of observations for *hottest days, hottest nights* and *coldest nights*. This shows that for these indices there is greater certainty in comparison to observations. The *coldest nights* index is the only exception; the model shows less certainty than observations by having broader confidence intervals that overlap zero. This uncertainty is likely related to the high interannual variability (Table 3.3) simulated by the model for this index.

3.2.4 Variability

Dataset	TXx	TNx	TXn	TNn
GHCNDEX	0.62	0.69	0.90	0.88
GHCN	0.63	0.68	0.87	0.69
HQ	0.66	0.74	0.92	0.77
HadGHCND	0.67	0.71	0.88	0.79
HadEX1	0.75	0.73	0.93	0.88
HadEX2	0.65	0.75	0.96	0.79
AWAP	0.67	0.78	0.96	0.75
Mk3L (model)	0.45	0.53	1.54	0.60

Table 3.3: The standard deviations of Australian averaged time series for period the 1957 to 2000, according to each dataset and the model. The standard deviation is calculated for each index (Table 2.1) using only grid boxes containing observations common to all datasets. Units are °C.

Standard deviations of time series (Figure 3.2) are calculated and analysed for further

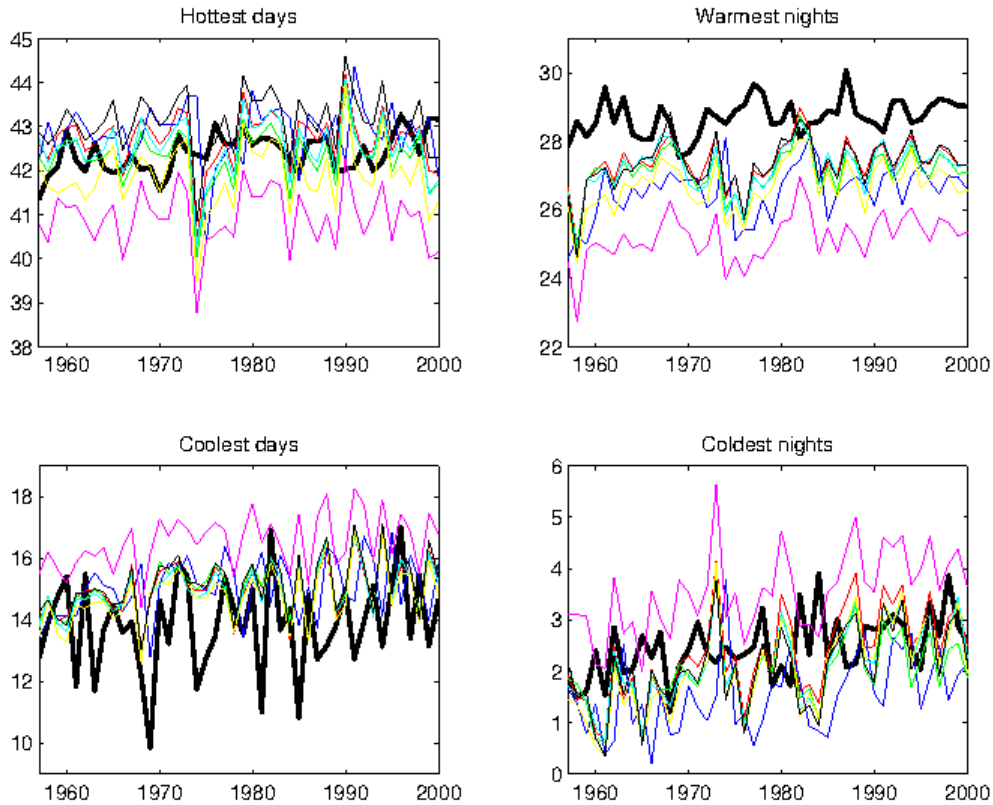


Figure 3.2: Temperature ($^{\circ}\text{C}$) of *hottest days* (TNn), *hottest nights* (TNx), *coldest days* (TXn) and *coldest nights* (TNn) from 1957 to 2000 averaged over Australia using grid squares containing observations common to all datasets. Red = GHCN-DEX, Green = GHCN AUS, Light Blue = HQ AUS, Pink = HadGHCND, Yellow = HadEX1, Thin Black = HadEX2, Blue = AWAP, Thick Black = Mk3L.

assessment of variability, recorded in Table 3.3. Compared to observations the model slightly underestimates year-to-year variability of all indices except the *coldest days* index which displays more variability than observations. *Coldest days* is also the most variable index across the model and observations, followed by *coldest nights*. Less variable than these two indices, *hottest days* and *hottest nights* have comparable variability. The model agrees with observations that *coldest days* displays the largest interannual variability followed by *coldest nights*. Observations show *hottest nights* exhibits the third highest interannual variability followed by *hottest days*, whereas the relative variability exhibited by these two indices within the model is reversed.

3.3 Summary of model evaluation

Differences in the magnitude of the trend may be the result of decreased or increased year-to-year variability of the model relative to observations. The model seems to have least skill reproducing the variability of *coldest days*; this index had a high degree of variability relative to observations (Figure 3.2 and Table 3.3). The model does well capturing variability for *hottest days*, *hottest nights* and *coldest nights* and only slightly underestimates the variability of these indices.

The model overestimates temperature for the *hottest nights* index (Figure 3.2). The model is most skillful at reproducing the temperature magnitude of *hottest days and coldest nights*. The model is also very capable at capturing trends for *hottest nights, coldest days and coldest nights*. Spatially the model does well and generally does not differ from observations by more than $\pm 5^{\circ}\text{C}$ (Figure 3.1).

Relative to simulated mean temperature using state of the art CMIP5 models (not presented here), the model produces very pleasing results (Sillmann *et al.*, 2012). Mean temperatures are much easier to reproduce than extremes and, considering the model's coarse resolution, it appears capable of reproducing observational temperature extremes. Moreover, Mk3L performs competitively and improves on the ability of many, if not all of the CMIP3 models to reproduce temperature extremes (Perkins *et al.*, 2007; Alexander & Arblaster, 2009); although Alexander & Arblaster (2009) did not assess exactly the same indices used here.

The model successfully reproduces the trend, variability, and intensity of all indices. Across all measures assessed here, the model does not vary from the observations by more than the observational datasets vary amongst themselves.

Chapter 4

Results

The results section is structured along the lines of the following questions:

1. How does internal variability drive temperature extremes? (Section 4.1)
2. How do external forcings drive temperature extremes? (Section 4.2)
3. How do solar and volcanic forcings act together to drive temperature extremes? (Section 4.3)
4. How do anthropogenic forcings drive temperature extremes? (Section 4.4)
5. What is the overall variability of temperature extremes? (Section 4.5)

4.1 Internal variability

This study primarily assesses the role of external drivers on temperature extremes in Australia. To varying degrees extreme indices are also influenced by internal climate drivers. Here, initial analysis turns to identifying relationships between dominant modes of internal climate variability and temperature extremes in Australia. This approach uses simulation OGSV as the most realistic simulation of the real world. Figure 4.1 shows the

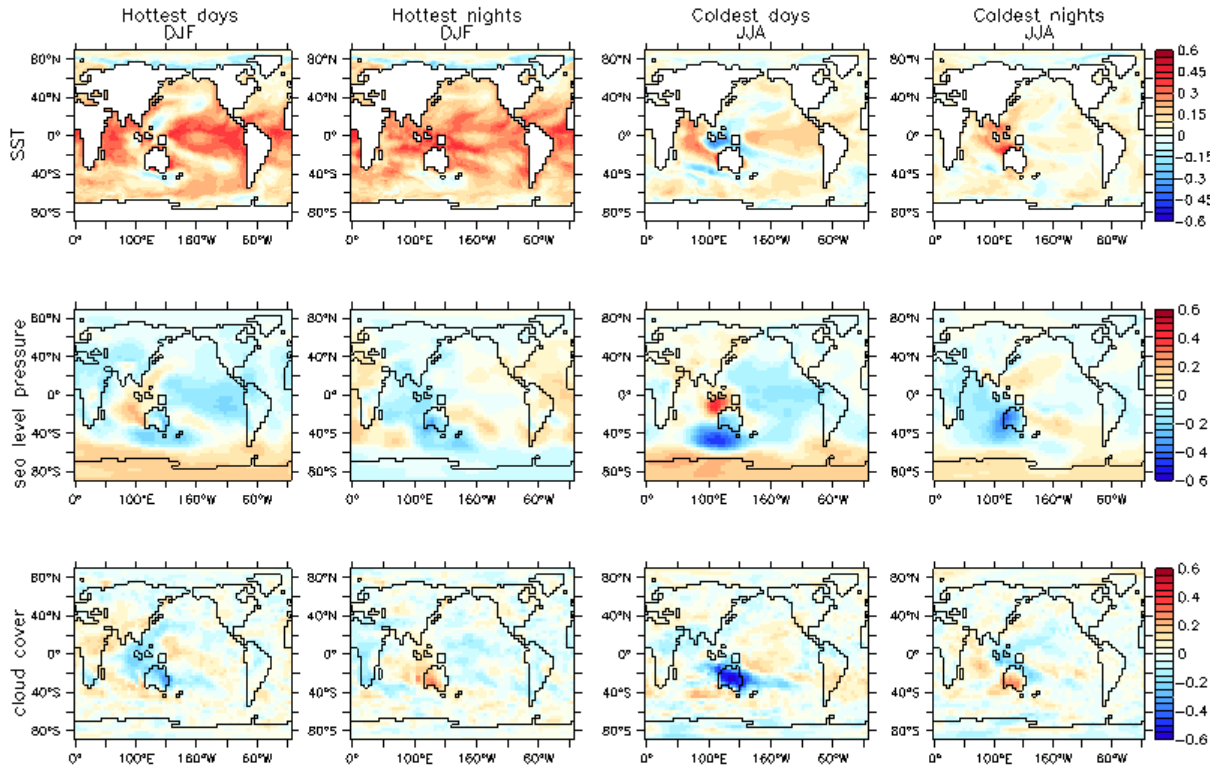


Figure 4.1: The correlation between the magnitude of annual Australia averaged temperature extremes and seasonal means in sea surface temperature, sea level pressure and cloudiness, according to simulation OGSV over the pre-industrial period (1001 to 1850). Correlations are calculated with summer (December January February (DJF)) for T_{max} indices and winter (June July August (JJA)) for T_{min} indices.

correlations between temperature extreme indices and the seasonal averages in sea surface temperature (SST), sea level pressure (SLP) and cloudiness for the period 1001 to 1850. T_{min} indices were correlated against winter variables (June July August (JJA)); whereas T_{max} indices were correlated against summer variables (December January February (DJF)). Correlations between temperature indices (Table 2.1) and mean SST in the Niño 3, 3.4 & 4 regions, Indian Ocean Dipole (IOD) and cloudiness over Australia are given in Table 4.1 and Table 4.2. Assessment of Figure 4.1 led to the singling out of these internal climate variables for a more detailed appraisal of the modes within the ocean-atmosphere system that are driving extremes in Australia.

The IOD is measured using the Dipole Mode Index (DMI) (Saji *et al.*, 1999). The DMI is defined as the SST gradient between the western equatorial Indian Ocean (50°- 70°E, 10°S - 10°N) and the south eastern equatorial Indian Ocean (90°- 100°E, 10°S - 0°S). Niño region indices (Trenberth, 1997) are calculated as the seasonal area averaged SST (°C) for the specified region. Niño 3 (150°- 90°W, 5°S - 5°N), Niño 3.4 (170°- 120°W, 5°S - 5°N) and Niño 4 (160°E - 150°W, 5°S - 5°N) regions are calculated.

An ENSO signal is more evident in T_{max} indices rather than T_{min} and exhibits the strongest relationship with *hottest days*. Interdecadal Pacific Oscillation (IPO) and Pacific Decadal Oscillation (PDO) patterns are evident in all extreme indices but the signals are weak and do not show a particularly strong relationship with any index. All four extreme indices exhibit correlations with local SST, however T_{max} exhibit particularly strong correlations relative to T_{min} (Figure 4.1). The only strong correlations between SLP and temperature indices are associated with T_{min} indices.

Correlations are calculated between extreme temperature indices and seasonal Australia averaged cloudiness. During the day, clouds reflect shortwave radiation, restricting the amount of solar radiation to reach the Earth's surface and therefore cooling temperatures. During the night, clouds have the opposite effect, trapping longwave radiation and causing the Earth's surface to warm. The effects of cloudiness on surface temperature are also dependent on many other variables associated with cloud type, height within the troposphere, density etc (Dai *et al.*, 1999).

4.1.1 Hottest days

An ENSO signal is evident in *hottest days* and reasonable correlations exist with the Niño 3, 3.4 & 4 regions. Of these relationships, it is evident that the strongest signals lie

Indices	TX _x	TN _x
Niño 3	+0.34	+0.26
Niño 3.4	+0.29	+0.19
Niño 4	+0.33	+0.21
DMI	+0.23	-0.03
Aust. cloudiness	-0.27	+0.19

Table 4.1: The correlation between the magnitude of annual Australia averaged temperature extremes and DJF SST means in the Niño 3, 3.4 & 4 regions, DMI and Australia averaged cloudiness.

Indices	TX _n	TN _n
Niño 3	+0.18	+0.06
Niño 3.4	+0.18	+0.06
Niño 4	+0.22	+0.05
DMI	+0.28	-0.15
Aust. cloudiness	-0.61	+0.19

Table 4.2: The correlation between the magnitude of annual Australia averaged temperature extremes and JJA SST means in the Niño 3, 3.4 & 4 regions, DMI and Australia averaged cloudiness.

with Niño 3 and Niño 4. These correlations are almost equal during both summer (DJF) and winter (JJA - not shown) but strongest during DJF. The Niño 3 region explains 12% ($r^2 = 0.12$, where $r = +0.34$); and likewise the Niño 4 region explains 11% ($r^2 = 0.11$, where $r = +0.33$), of the interannual variability of *hottest days* (Table 4.1). Whilst these correlations are not particularly strong, these are the strongest relationships common to the internal indices assessed here and *hottest days*. *Hottest days* are correlated with cloudless days, but this relationship is not particularly strong, maintaining 7% ($r^2 = 0.07$, where $r = -0.26$) of mutual interannual variability.

4.1.2 Hottest nights

Whilst strong correlations exist between *hottest nights* and SST, the patterns of the responsible dynamical modes are less obvious. *Hottest nights* does not exhibit strong correlations with other variables (SLP or cloudiness; Figure 4.1). *Hottest nights* is correlated to the Niño regions assessed here (Table 4.1), suggesting an ENSO-like relationship with similar correlations during winter (JJA - not shown). However, the lack of a dominant ENSO-like pattern in Figure 4.1 shows that other modes are also important, as

similarly strong correlations are evident in many other regions.

4.1.3 Coldest days

Cloudiness is very highly correlated with *coldest days* relative to the other extreme indices. *Coldest days* are found to share 38% of variability ($r^2 = 0.38$, where $r = -0.61$) with the high cloudiness region over Australia. This correlation indicates that the variability of *coldest days* is largely (38%) characterised by the variability of cloudiness (an internal climate forcing).

Coldest days also demonstrates an IOD signal (Figure 4.1). The correlation between the Dipole Mode Index and *coldest days* is 0.28, describing 8% of the variance for this index (Table 4.2). *Coldest days* negatively correlates with a high pressure zone in the southeast Indian Ocean and positively correlates with a low pressure zone in the northeast Indian Ocean over Indonesia.

The variability in IOD and cloudiness can account for almost half of the variability exhibited by *coldest days*. Across all extreme indices assessed, *coldest days* maintains strong (either negative or positive) correlations across all three climatic variables considered here (SST, SLP and cloudiness), indicating that internal climate drivers have a substantial relationship with the variability of this index. The relatively large number of strong correlations identified across these variables, associated with and accordingly driving this index, demonstrate the reason for its large interannual variability.

4.1.4 Coldest nights

Figure 4.1 shows a relationship between the *coldest nights* index and high SLP over a broad region spanning Western Australia and the Indian Ocean. This region coincides with the region where *coldest nights* correlates with low cloudiness (Figure 4.1). The temperature gradient over the equatorial Indian Ocean gives rise to a small relationship with the IOD (Table 4.2).

Whilst some relationships are evident between the variability of ocean-atmosphere variables and *coldest nights* (Figure 4.1), the index maintains relatively low correlations with all area averaged correlations assessed here (Table 4.1 and Table 4.2). Few relationships are identified between specific modes of variability and *coldest nights*.

4.1.5 Summary of internal variability

Hottest days variability is highly correlated to equatorial and local SST, particularly ENSO and Niño regions 3 & 4. Cloud cover during the night relates to warm nights and cold days as expected and the vice versa. This relationship holds true for all extreme temperature indices assessed here. The IOD maintains a strong relationship with *coldest days* and also, hottest days, to a lesser extent. *Coldest days* maintain high correlations with many variables, suggesting this index is strongly influenced by internal climate drivers, some of which were not able to be defined. Similarly, *coldest nights* exhibits many high correlations but, on the other hand, few of these relationships are able to be traced to particular climatic modes. Other internal modes are likely to be contributing drivers to all indices even though they weren't able to be identified through the assessments performed here (Figure 4.1, Table 4.1 and Table 4.2).

4.2 External drivers

This study now turns to understanding the role of external drivers on temperature extremes in Australia over the past 1000 years. In this case, external drivers refer to volcanic (Section 4.2.1) and solar (Section 4.2.3) forcings and how they interplay (Section 4.3). The structure of Section 4.2 and Section 4.1 are not analogous because the behaviour of internal forcings are often intertwined and their influence varies largely from index to index, in contrast to external forcings, where large differences arise between forcings themselves.

4.2.1 Volcanic eruptions

Figure 4.2 shows the time series of simulation OGV and simulation OGSV (Table 2.2). Signals from all three volcanoes assessed here (Table 2.3) are evident in the OGV and OGSV time series and are anomalous relative to the pre-industrial mean (Figure 4.2a & b, respectively). The volcanic eruption of 1258 exhibits a similar response to Tambora (Figure 4.2b) even though 1258 produced a larger radiative forcing anomaly (Table 2.3).

Subtracting simulation OG from simulation OGV isolates the influence of volcanism from other forcings and allows forcing specific analysis to be performed. To robustly capture the volcanic signal and reduce the influence of internal interannual variability, a composite of eruptions was used for assessment. Refer to Figure 4.3 for time series of OGV minus OG, averaged over Australia. The time series composite reveals large, abrupt and statistically significant cooling of *hottest days*, *hottest nights* and *coldest nights*. In all cases cooling occurs abruptly; in the year subsequent to volcanic eruptions. The influence of volcanic eruptions on *hottest nights* and *coldest nights* is longer lived relative to *hottest days* with statistically significant cooling still present in the fourth year after

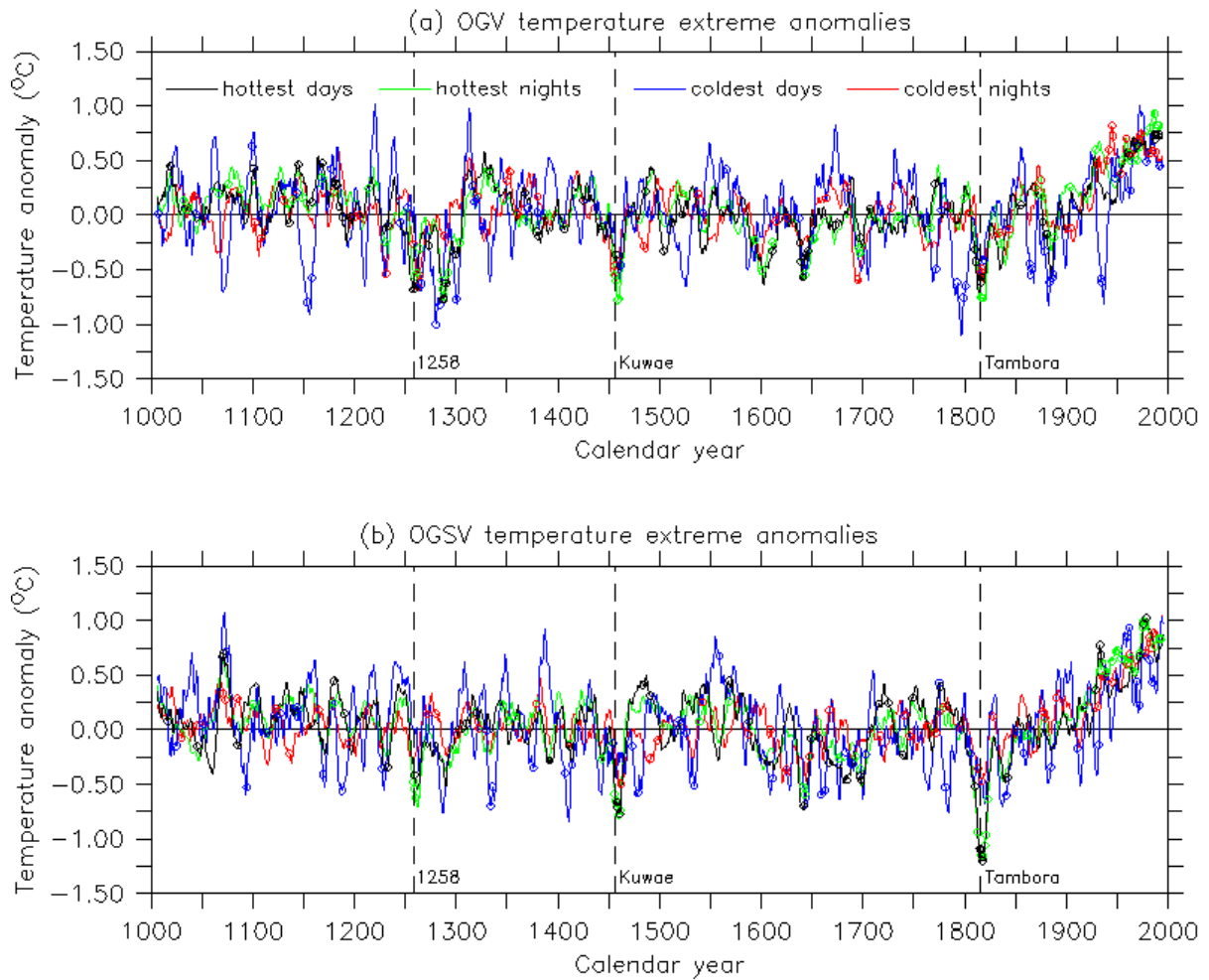


Figure 4.2: Changes in temperature extremes over the last millennium relative to the pre-industrial mean. (a) Simulation OGV and (b) simulation OGSV, respectively, expressed as 10 year running means. Statistical significance at the 5% level is denoted by circles.

eruption. Considering the magnitude of cooling, *hottest nights* cools most followed by *hottest days* and *coldest nights*. No influence is identifiable for *coldest days*.

Considering the longevity of the volcanic signal in temperature extremes, the year of eruption plus the subsequent two calendar years is used to further assess the influence of volcanism on extremes. Again, a composite of eruptions is used to objectively capture the volcanic signal by improving the signal to noise ratio. This produces a composite of nine calendar years, which is used to assess spatial variations (Figure 4.4).

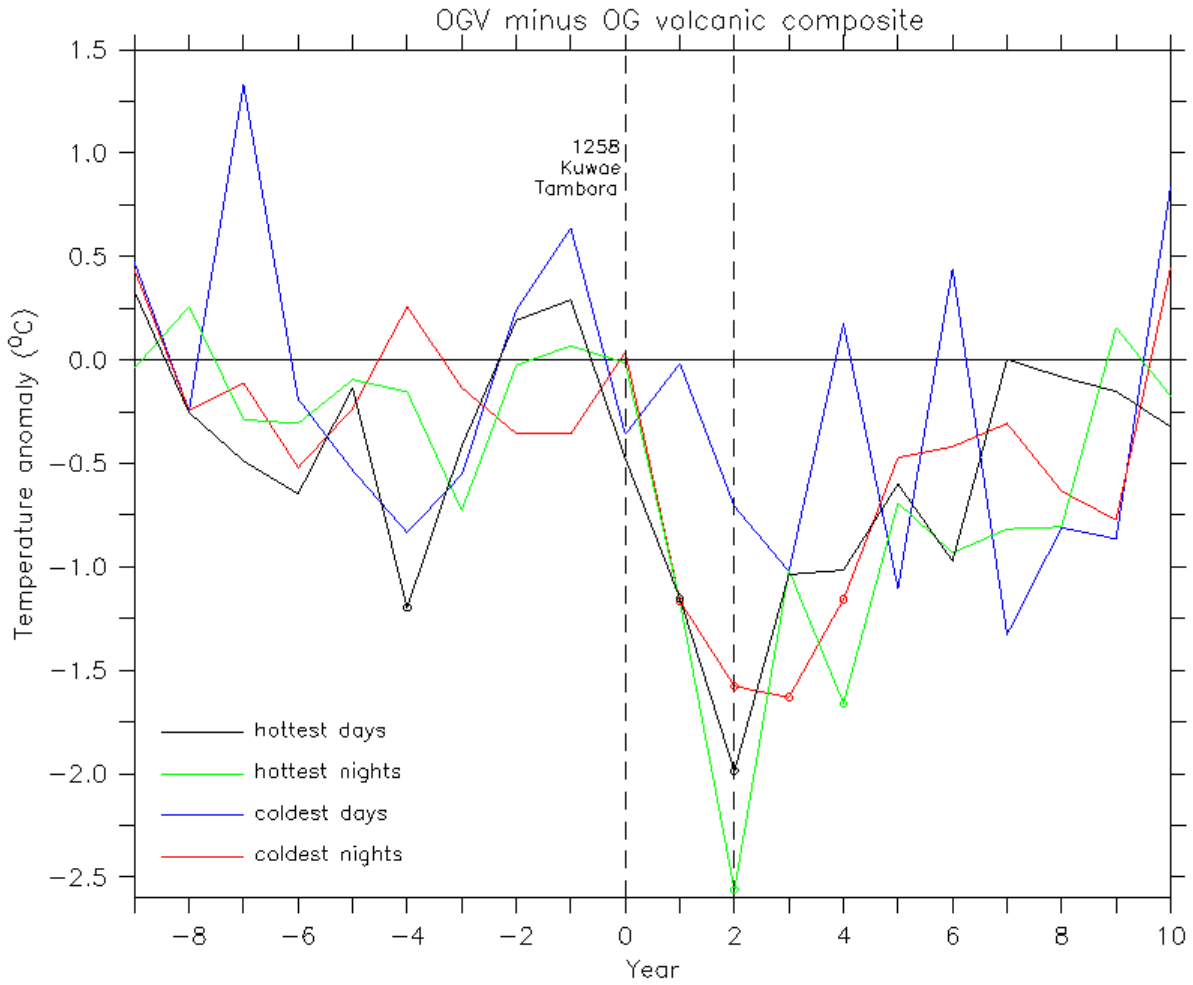


Figure 4.3: Composite of OGV minus OG (refer to Table 2.2 for explanation of simulations) of the three largest eruptions with a twenty year window: 1248-1268, 1446-1466, 1806-1826. Year zero represents 1258, 1456 and 1816 simultaneously; year 10 represents 1268, 1466, 1826 etc. Circles denote statistical significance at the 5% level.

All indices that are influenced by volcanism (*hottest days*, *hottest nights* and *coldest nights*) yield large temperature changes of at least 2.5°C (Figure 4.4). The spatial distribution of the temperature change is different for each index. However, the number of grid boxes to undergo significant cooling is comparable for each index. Across all indices that experience significant cooling, the coastal region of eastern Australia cools least. Still, across all indices, significant cooling occurs in almost every grid box. Tasmania experiences significant cooling for the *hottest nights* index only. On a grid point by grid

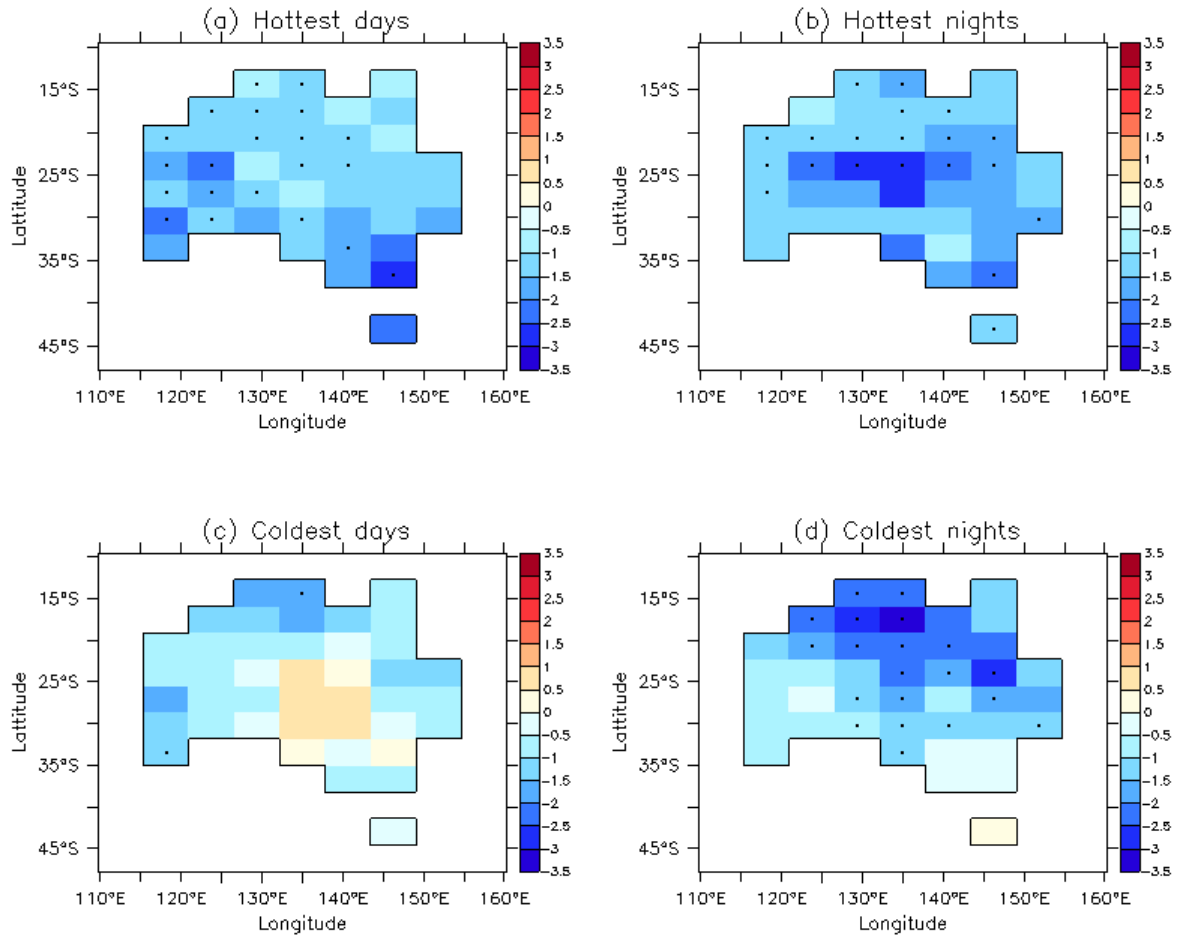


Figure 4.4: Composites of simulation OGV minus simulation OG of three largest volcanic eruptions (Table 2.3) for each extreme temperature index. Stippling indicates significance at the 5% level. Units are $^{\circ}\text{C}$.

point basis, *coldest nights* cools most (3.1°C). Alternatively, averaged across Australia, *hottest nights* undergoes the largest cooling (2.6°C). The cooling for *hottest nights* is more uniform across Australia compared to the other indices. The *coldest nights* index on the other hand undergoes more extreme but localised changes.

No volcanic eruption, regardless of amplitude, was found to influence the *coldest days* index. No (significant) change in magnitude or behaviour of *coldest days* were found in the years subsequent to an eruption.

4.2.2 Summary of volcanic forcing

Volcanic eruptions significantly influence the extremity of *hottest days*, *coldest nights* and *hottest nights* indices. *Hottest days and nights* become less extreme. *Coldest nights* become more extreme and *coldest days* are not influenced. Volcanic eruptions have a dramatic, but brief influence on temperature extremes (one to four years).

4.2.3 Solar Irradiance

Anomalies of temperature extremes within forced simulation OGS exhibit warming early in the millennium (Medieval Climate Anomaly) and a slight cooling in the seventeenth century (Little Ice Age), coinciding with periods of relatively high and low solar irradiance, respectively (Figure 2.1). These are less evident in simulations involving volcanic eruptions (Figure 4.2). However, it is questionable whether these features are related to fluctuations of TSI as these features remain identifiable under OG forcing only (Figure 4.5b). Temperature extremes forced by OG give rise to larger centennial scale variability during the pre-industrial era. Thus, temperature extreme anomalies may not be forced by solar variability as they are also evident in simulation OG but may be more obvious due to the lack of other centennial scale variability.

The Maunder Minimum (MM) is analysed in further detail, being the period of lowest solar insolation without a major volcanic eruption. No significant changes to the temperature extremes between simulations, OGS and OG, are identified during the MM (Figure 4.6). Analysis of the period with lowest solar insolation, the Spörer Minimum (1460-1550), does not reveal statistically significant changes to temperature extremes (not shown), relative to both mean pre-industrial extremes and simulation OG.

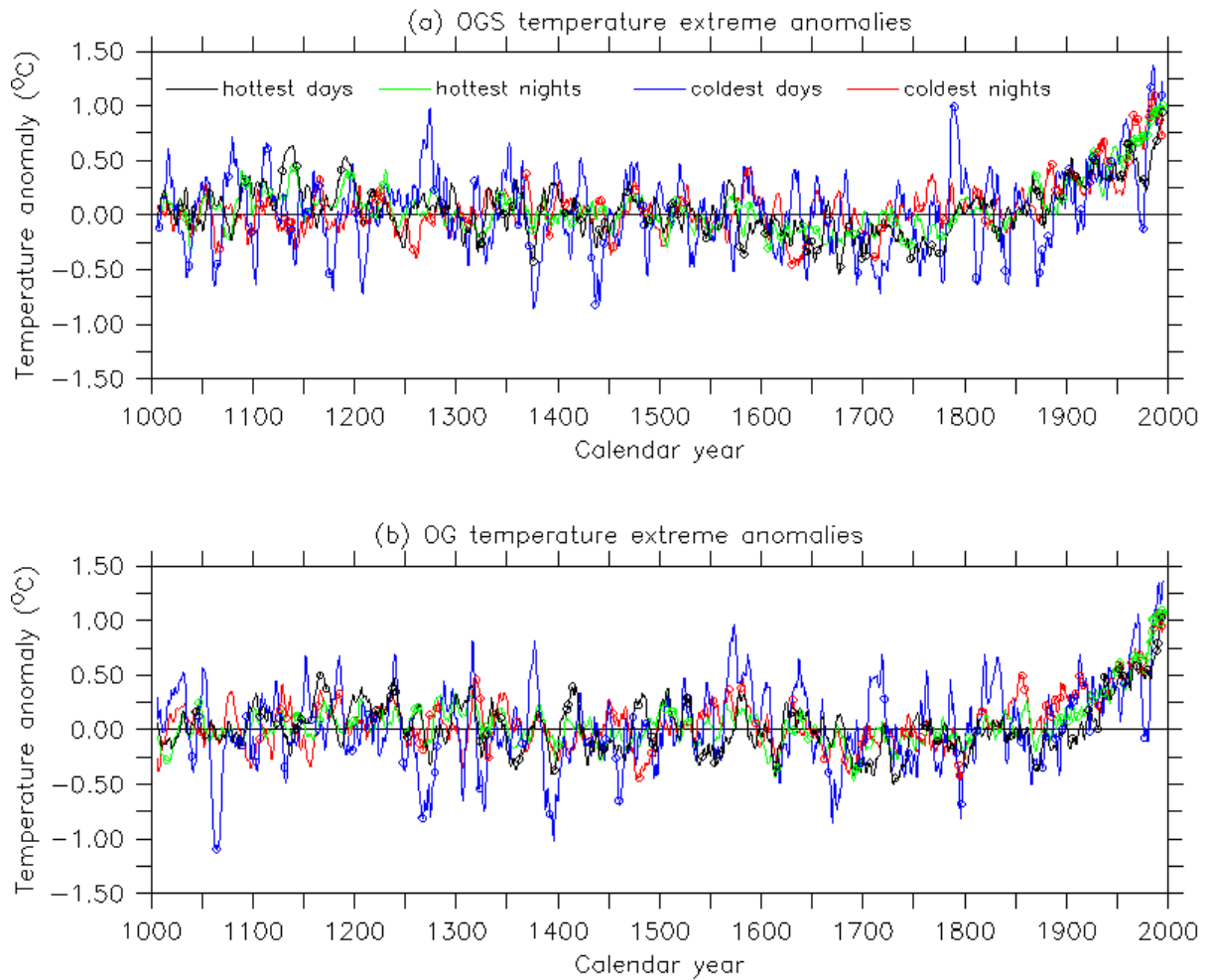


Figure 4.5: Changes in temperature extremes over the last millennium relative to the pre-industrial mean. (a) Simulation OGS and (b) simulation OG, expressed as 10 year running means. Statistical significance at the 5% level is denoted by circles. Units are $^{\circ}\text{C}$.

4.2.4 Summary of solar forcings

No significant changes to any temperature extreme indices were found through analysis of direct comparisons between OGS and OG simulations (Table 2.2) over the MM (1645 to 1715); nor comparisons between the MM and the pre-industrial period.

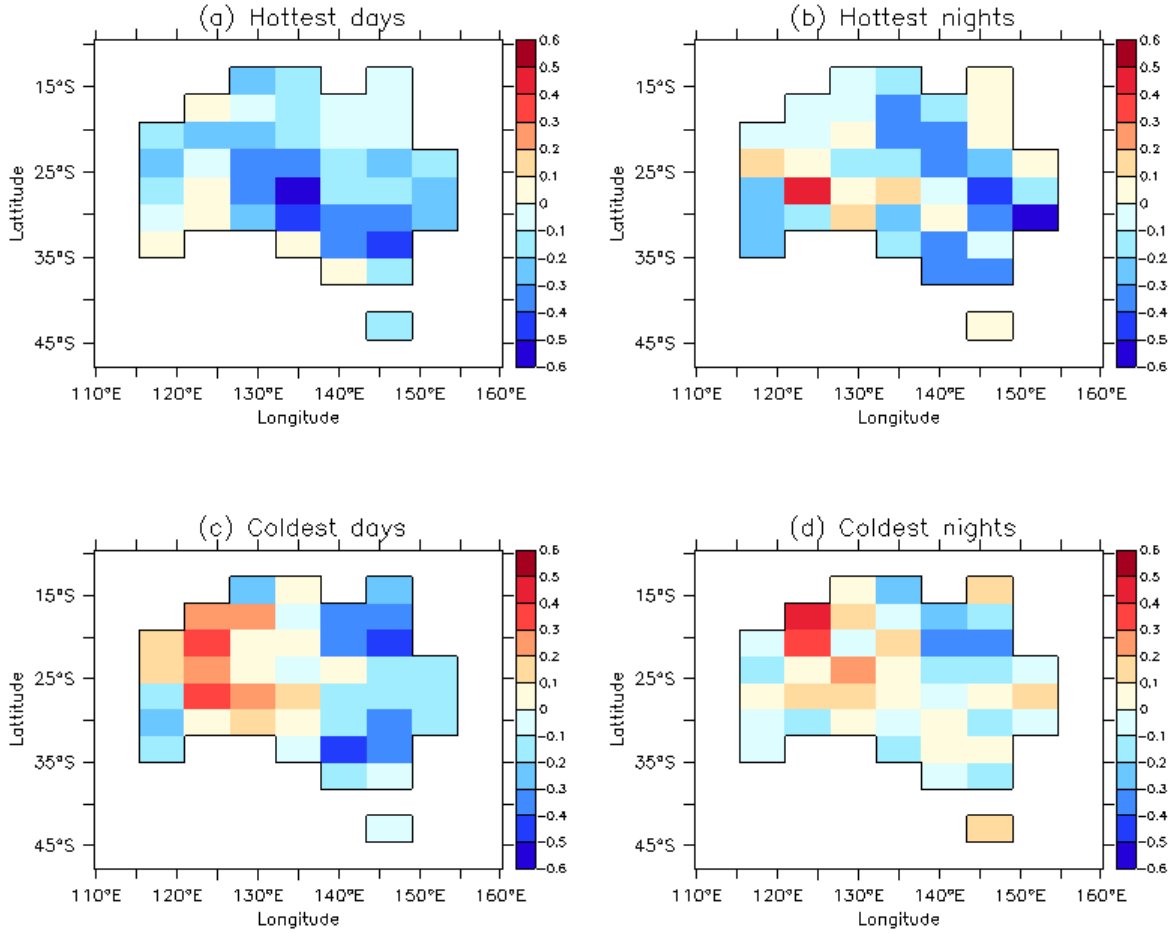


Figure 4.6: Simulation OGS minus simulation OG for each extreme temperature index (Table 2.1) during the Maunder Minimum (1645 to 1715). No statistically significant values were found at the 5% level. Units are °C.

4.3 Dynamic duo; volcanic and solar forcings

All three volcanoes (Table 2.3) are evident in the time series of simulations OGV and OGSV (Figure 4.2). Close analysis of these time series puts perspective on the combined influence of total solar irradiance (TSI) and volcanism. Within simulation OGV and generally across indices, the largest eruption, 1258, exhibits the largest anomalous cooling, Tambora exhibits the second largest anomalous cooling and Kuwae the third largest anomalous cooling. Within OGSV, Tambora exhibits the largest cooling, followed by

Kuwae and 1258, which cool comparably. Of the three volcanic eruptions; 1258 occurred during the MCA, Kuwae during the Spörer Minimum (SM) and Tambora within the LIA.

Simulation OGSV results in greater cooling of T_{max} subsequently Tambora, relative to simulation OGV. *Hottest days* exhibits greater cooling and is the only index to undergo significant change following Kuwae in simulation OGSV relative to OGV. 1258 does not exhibit uniform changes and the only index influenced by the inclusion of solar forcing in OGSV relative to OGV is *coldest nights*, which cools less. Comparing the three volcanic eruptions (Table 2.3), T_{max} experiences greater cooling subsequent to Kuwae and Tambora, whereas *coldest nights* experiences less cooling subsequent to 1258 relative to simulation OGV (comparing Figure 4.2a & b). Whilst TSI does not have a direct impact on temperature extremes, comparisons between simulations OGSV and OGV, shows that fluctuations in TSI may enhance or reduce the impact of volcanic eruptions. To test this hypothesis, analyses performed in Section 4.2.1 are repeated using simulation OGSV.

Comparing Figures 4.3 and 4.7, the signal from volcanic eruptions persists longer in simulation OGSV relative to OGV only. *Hottest nights* reaches maximum cooling later in simulation OGSV relative to simulation OGV. Continuous, statistically significant, decreased temperatures experienced by *hottest nights* is extended following an eruption to experience significant cooling in the sixth year following eruption. *Hottest days* also cools for longer and endures significant cooling in the sixth year following a volcanic eruption. Thus, T_{max} indices are similarly influenced by volcanic eruptions when the model is forced with OGSV. The cooling experienced following an eruption is extended for T_{max} indices in the presence of volcanic and solar forcings (OGSV) relative to volcanic only (OGV).

However, the signal of volcanic eruptions on *coldest nights* is delayed and the longevity

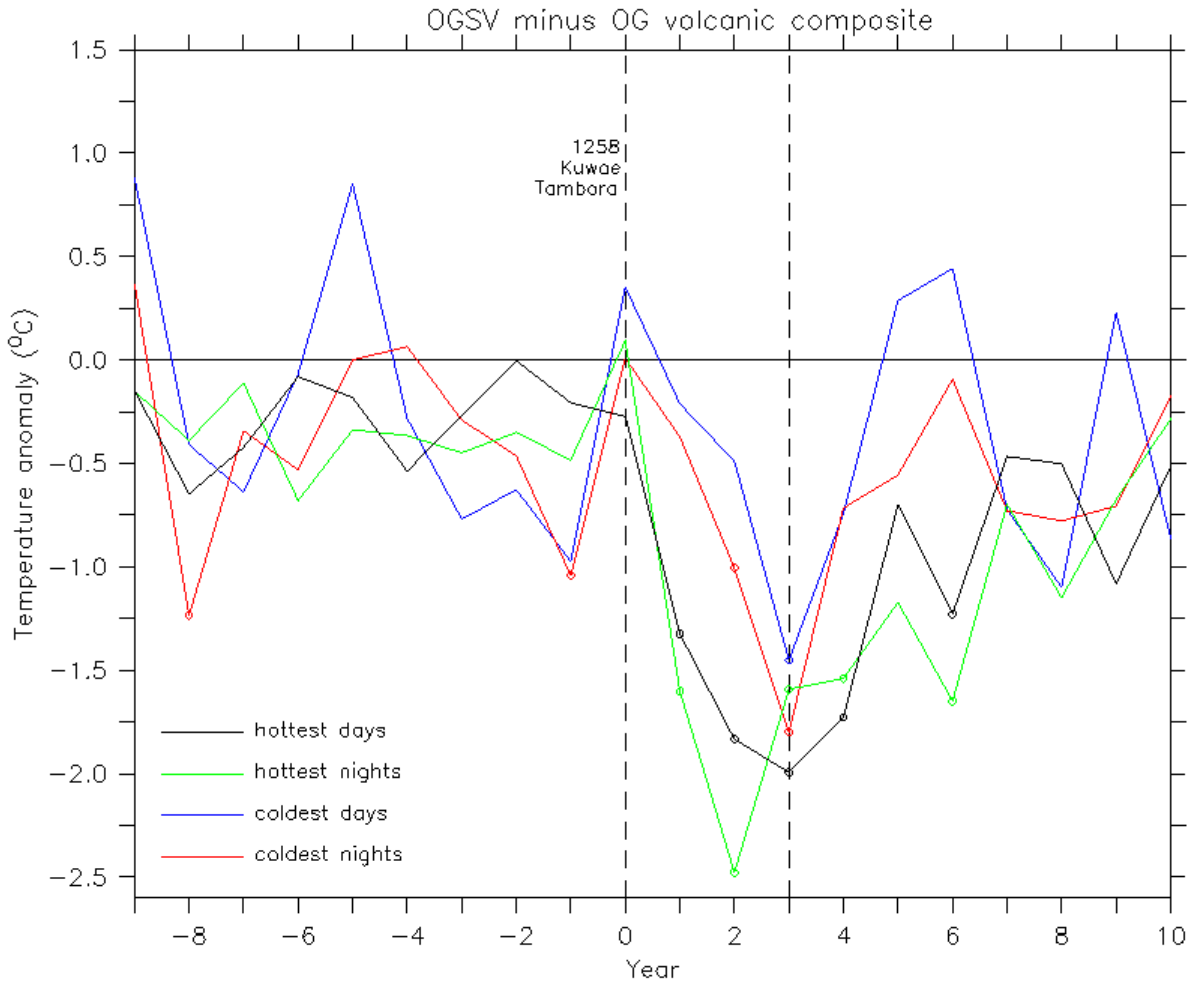


Figure 4.7: The composite of OGSV minus OG for the three largest volcanic eruptions of the millennium with a twenty year window: 1248-1268, 1446-1466, 1806-1826. As in Figure 4.3 but for simulations, OGSV minus OG.

reduced with the inclusion of solar forcing. This index is not impacted upon until later following eruptions and exhibits half the number of statistically significant anomalous points (which are annual extremes). The *coldest days* index does cool subsequent to volcanic eruptions, as is evident in Figure 4.7 & the three eruptions in Figure 4.2b. However, it is not possible to say that this is related to volcanism, due to the high year to year variability exhibited by this index (Figure 4.12) and the lack of grid points that undergo statistically significant cooling following eruptions (Figure 4.8). Almost all grid boxes of the T_{max} indices cool significantly over the three year window chosen to assess

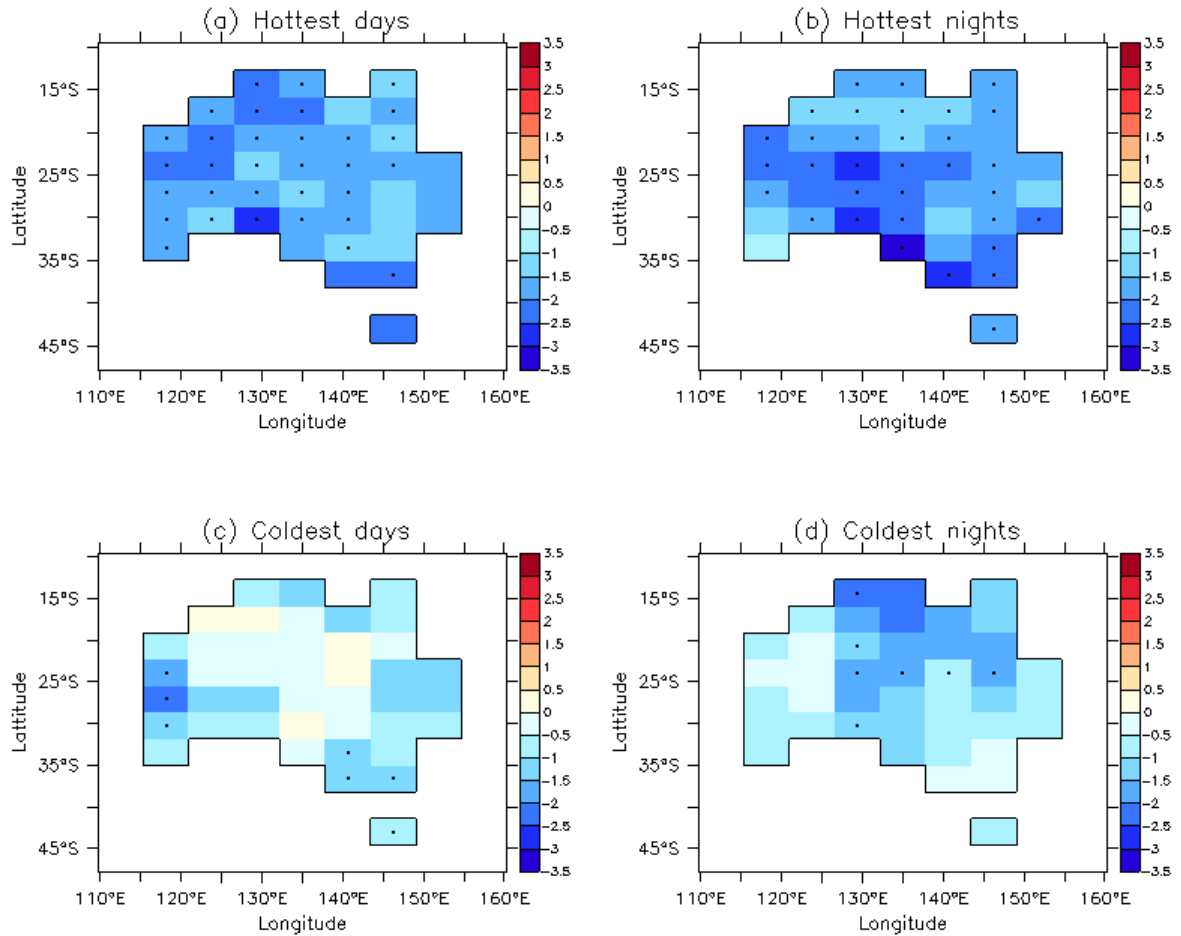


Figure 4.8: As Figure 4.4 but for simulations, OGSV minus OG. Units are °C.

the spatial influence of volcanism on temperature extremes. The east coast is a less influenced area of Australia (Figure 4.8), analogous to the OGV results (Figure 4.4). In Tasmania the extremity of *hottest nights* index declines significantly under both OGSV and OGV forcings subsequent to eruptions. Tasmania is also subjected to large decreases in extreme temperatures for *hottest days* but this is not statistically significant. Forced by OGSV, *coldest nights* has few grid points that undergo significant change, dissimilar to the OGV results (Figure 4.4). Solar forcing strengthens the influence of volcanic eruptions on T_{max} indices and weakens the influence of volcanic eruptions on *coldest nights* (T_{min}).

4.3.1 Summary of dynamic duo

A significant change is not observed in temperature extremes during periods of solar fluctuation under OGS forcings. However, solar forcing does alter the behaviour of extreme temperature indices following volcanic eruptions. The presence of solar forcings during volcanic eruptions has varying impacts on extreme temperature indices. T_{max} deviations were extended, whereas *coldest nights* deviations were abridged. The *coldest days* index is not impacted upon by volcanic eruptions (simulation OGV) or anomalous TSI (simulation OGS) but a volcanic signal is evident in simulation OGSV. Solar forcing is found to have little influence on temperature extremes but enhances (or reduces) and temporally extends (or shortens) the impact of volcanic eruptions on temperature extremes.

4.4 Anthropogenic drivers

Figure 4.9 shows the ten year running mean of the orbital only (O) simulation annual temperature extreme anomalies relative to the pre-industrial period for each index averaged over Australia. When orbital forcing alone is applied to the model, no long-term trend is evident. The addition of greenhouse gases gives rise to a clear and large warming trend during the industrial period (Figure 4.5). To determine the influence of anthropogenic forcing on annual temperature extremes, the recent period since industrialisation is compared to the millennium, and comparisons are made between forced experiments OG and O.

Coldest days remain highly variable (maintaining ± 0.8 °C) as they have done under all the forcings combinations (Table 2.2) applied to the model simulations (Figure 4.9). Within all simulations, *coldest days* exhibits greater variability relative to the other indices. Anomalies of other indices mostly lie between ± 0.4 °C throughout the millennium with

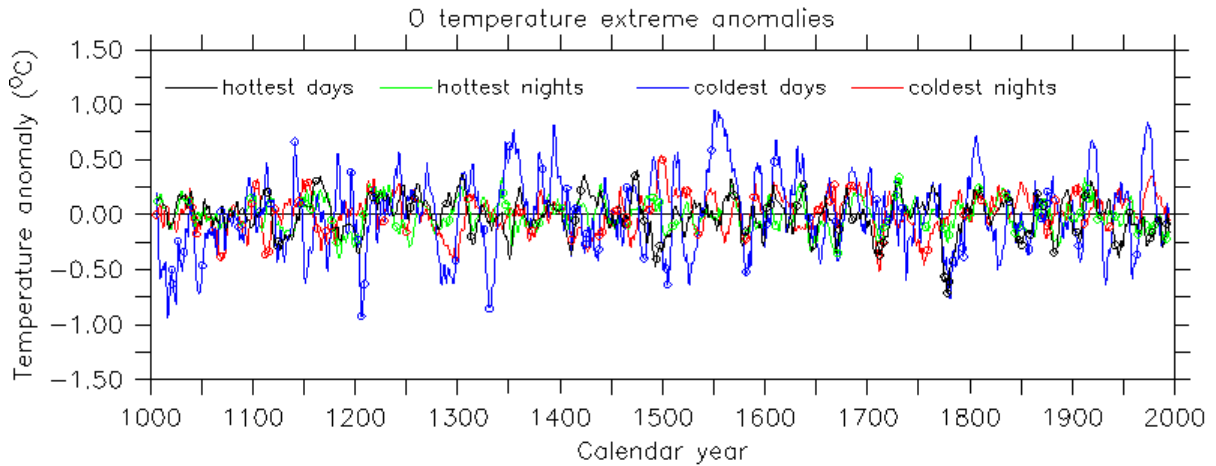


Figure 4.9: Annual temperature extreme anomalies over the last millennium relative to the pre-industrial mean. Forced by orbital (O) forcing only. Expressed as 10 year runnings means in °C. Statistical significance at the 5% level is denoted by circles.

no long term trends.

Time series and trends of temperature extremes for simulation OG and simulation O over the twentieth century are displayed in Figure 4.10. Anthropogenic GHG increase the magnitude of the temperature extremes and their trends for all indices relative to simulation O. Trends for all indices are larger when forced with OG relative to O. T_{max} indices hold the largest trends and trend differences between OG and O forcings. The *coldest nights* trend is consistently increasing throughout the century prior to 1990, where it experiences a sudden cooling. The increasing trend of *coldest nights* may be influenced by this sharp temperature decline in the last decade. *Coldest days* is the only trend under simulation OG that is not statistically significant and this is likely due to its large interannual variability. Trends and time series over 1957 to 2000 are given in Table 3.2 and Figure 3.2, respectively.

Anomalous values are calculated for each index and simulation. Anomalous events, such as those caused by changes in external forcings, may drive statistically significant anomalous values. Statistically significant anomalies are shown in Figure 4.2 for OGV and

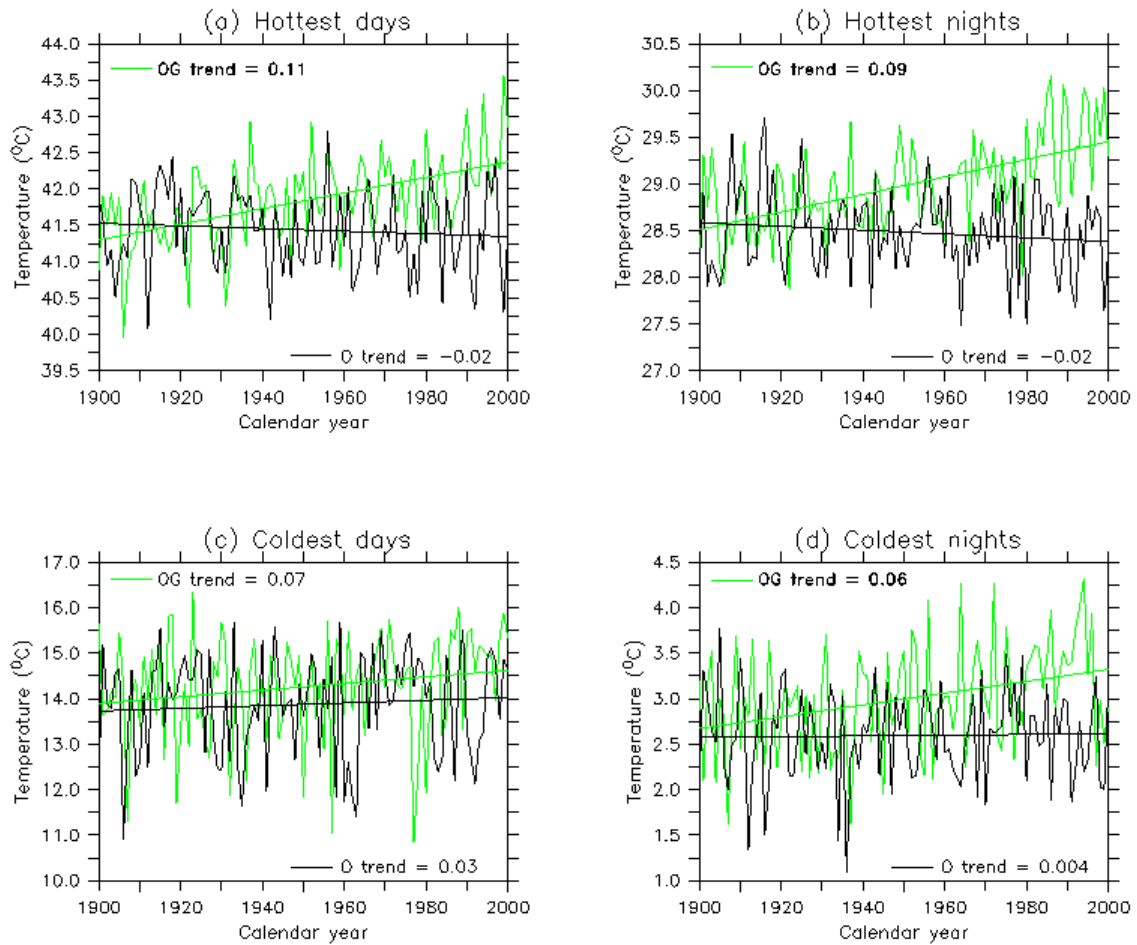


Figure 4.10: OG and O time series overlaid with the line of best fit over the twentieth century for temperature extreme indices averaged over Australia. Temperature (y axis) units are $^{\circ}\text{C}$. Trend units are $^{\circ}\text{C}$ per decade. Boldface signifies trends that are significant at 5% level.

OGSV forced time series; in Figure 4.5 for OGS and OG forced time series; and in Figure 4.9 for O forced time series. They reveal events or time periods where changes in external forcings have occurred.

The occurrence of significant values during the post industrial period (1970-2000) are used to assess the role (if any) greenhouse gases play in driving temperature extremes during this post industrial period (Table 4.3). A restricted post industrial time period was chosen (30 years) to maximise the ratio of the industrial time period relative to the

Forcing(s)	TXx	TNx	TXn	TNn
O	4%	4%	0%	4%
OG	12%	23%	2%	16%
OG:O	300%	550%	N/A	450%

Table 4.3: The percentage of annual extreme values that are statistically significant and fall between 1970 to 2000 as a percentage of the entire millennium. The ratio of statistically significant points of OG relative to O over 1970 to 2000 are shown as OG:O.

millennium. Measured in calendar years, the period 1970 to 2000 represents 3% of the millennium. In this respect, 3% of all statistically significant values would be expected to fall within this period.

O forced simulation gives rise to a scenario very similar to this (Table 4.3); statistically significant points for all indices fall between 0 and 4% of the millennium. When forced by OG, three of the four indices have more than 3% of their statistically significant extreme days fall during this industrial period. *Hottest nights* are most influenced by anthropogenic greenhouse gases (23%), followed by *coldest nights* (16%), *hottest days* (12%) and *coldest days* (2%). The sudden decrease in the magnitude of *coldest nights* after 1995 (Figure 4.10(d)) rains statistical significance but is more likely to be caused by internal variability than greenhouse gases and may therefore be amplifying and misleading the results of Table 4.3.

4.4.1 Summary of anthropogenic forcing

The inclusion of greenhouse gases increases the number of statistically significant extreme days. This demonstrates that greenhouse gases are a dominant driver of temperature extremes during this period with the exception of *coldest days*.

4.5 Variability of temperature extremes over the last millennium

It is necessary to assess the isolated influences of internal, external and anthropogenic forcings to gain a comprehensive understanding of their respective relationships with temperature extremes. However, in the climate system these forcings do not act in isolation but coexist with the potential to amplify and dampen each other whilst indirectly influencing temperature extremes through immeasurably complex relationships. Indeed, the influence of each forcing needs to be assessed in light of the entire climate system. Here we assess the differences between temperature indices considering influences from internal, external and anthropogenic forcings.

4.5.1 Inter-decadal variability

The large spread between simulations for the T_{max} indices (Figure 4.11) suggests that these indices are heavily influenced by external forcings. The spread between forced simulations of T_{min} indices (Figure 4.12) is much narrower, suggesting these indices are driven by internal variability rather than external forcings. Relative to *coldest days*, other indices maintain relatively similar year-to-year variability.

Comparing the standard deviations of temperature indices across simulations, the inclusion of solar forcing slightly increases the interannual variability of both T_{max} and T_{min} indices. While volcanism increases the interannual variability of T_{max} indices, it has little or no influence on T_{min} indices.

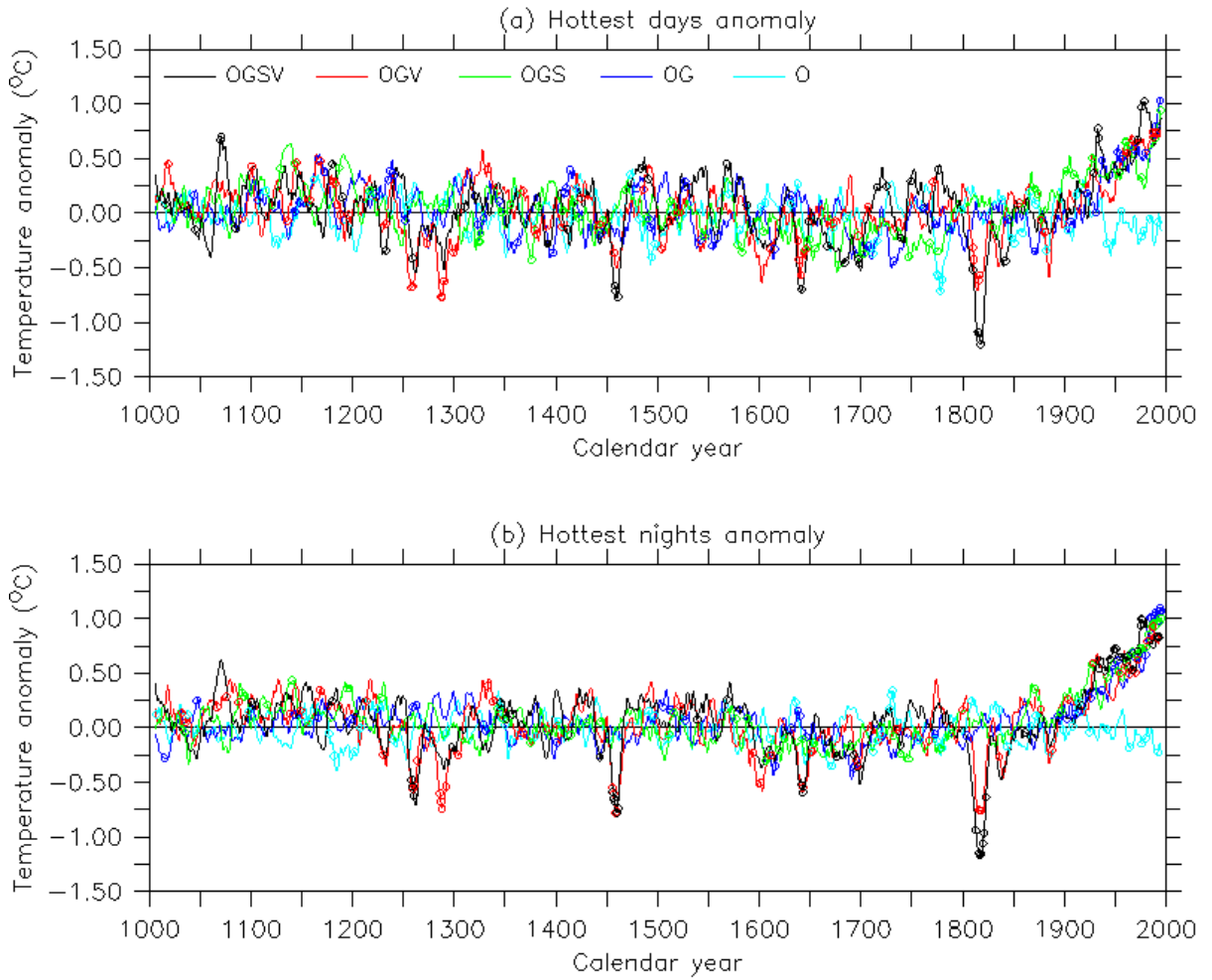


Figure 4.11: (a) Hottest days anomalies and (b) Hottest nights anomalies. The values shown are expressed as anomalies relative to the pre-industrial mean (1001 to 1850) for all forced simulations. Values for both plots are expressed in $^{\circ}\text{C}$ as 10 year running means. Circles denote statistical significance at the 5% level.

Forcing(s)	TXx	TNx	TXn	TNn
O	0.47	0.41	1.14	0.55
OG	0.50	0.41	1.16	0.56
OGS	0.51	0.42	1.09	0.54
OGV	0.58	0.51	1.11	0.56
OGSV	0.58	0.48	1.20	0.56

Table 4.4: Standard deviations of areally averaged time series for each temperature extreme index (Table 2.1) and model simulation (Table 2.2) from 1001 to 1850. Units are $^{\circ}\text{C}$.

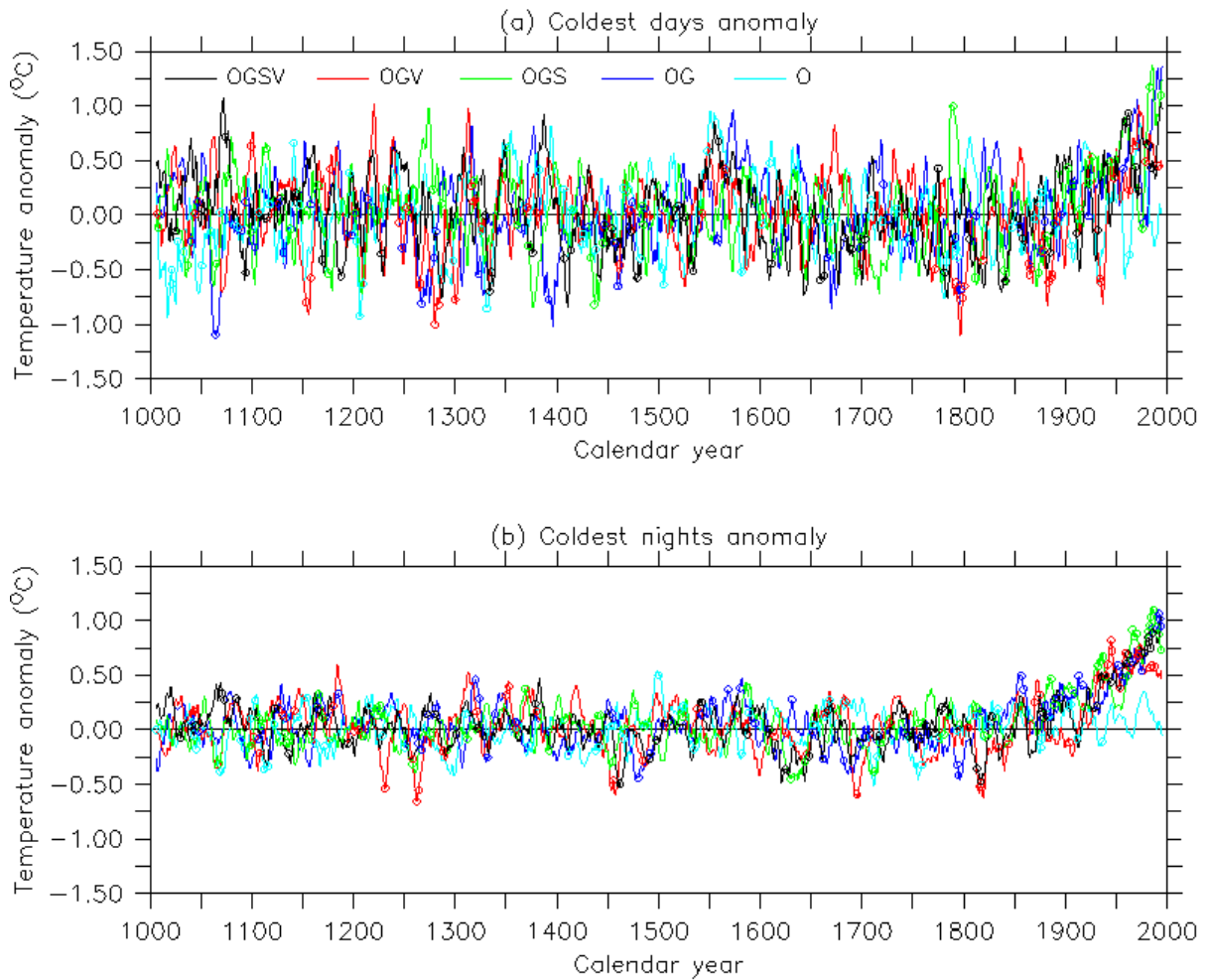


Figure 4.12: (a) Coldest days anomalies and (b) Coldest nights anomalies. The values shown are expressed as anomalies relative to the pre-industrial mean (1001 to 1850) for all forced simulations. Values for both plots are expressed in °C as 10 year running means. Circles denote statistical significance at the 5% level.

Hottest days

Hottest days matches the variability of *coldest nights* when forced with volcanism but otherwise exhibits less relative year-to-year variability. I have found that volcanism significantly influences *hottest days* and the extent of this influence is impacted upon by solar forcing. Although centennial scale changes due to changes in solar irradiance are observable, they are not statistically significant. From examination of the entire

millennium, it is clear that anthropogenic GHGs significantly increase the intensity of *hottest days*. *Hottest days* is also driven by internal climate variability (Section 4.1), particularly ENSO. Niño 3 & 4 regions play key roles in the interannual variability of *hottest days*.

Hottest nights

Hottest nights broadly behaves similarly to *hottest days*. However, *hottest nights* exhibits less interannual variability, maintaining the least interannual variability across all indices and simulations (Table 4.4). Relative to *hottest days*, *hottest nights* exhibits only slightly less year-to-year variability, with and without the inclusion of volcanism. Relative to *hottest days*, *hottest nights* is similarly influenced by volcanism, changes to solar irradiance, and increasing GHGs. However, *hottest nights* shows less breadth between simulations, suggesting that this index is less influenced by external forcings (Figure 4.11). Whilst it appears that the variability of *hottest nights* is at least to an extent related to the variability of internal climate drivers, no relationships between defined dynamical modes and this index were able to be identified.

Coldest days

Coldest days maintains the largest interannual variability and the least spread between simulations (Figure 4.12). Standard deviations of Australia averaged time series shows that the *coldest days* index exhibits by far the largest interannual variability relative to other indices (Table 4.4). This agrees with the assessments of internal climate variables (Section 4.1) and external drivers (Section 4.2) that *coldest days* either maintains a complex relationship with external climate drivers or is primarily driven by internal climate variability. The inter-decadal variability of *coldest days* is even more apparent

within simulations without solar forcing (O and OG). Assessment of internal climate drivers revealed that the interannual variability of *coldest days* is influenced by the IOD, cloudiness as well as maintaining high correlations with other variables where defined dynamical modes were not identified.

Coldest nights

Coldest nights exhibits the second highest interannual variability (Table 4.4) but is much less variable than *coldest days*. *Coldest nights* is marginally influenced by volcanism and this is dependent on solar irradiance. Internal climate dynamics such as IOD, SLP and cloudiness appeared to marginally influence *coldest nights*. Relative to *coldest days*, *coldest nights* exhibits a stronger signal from external forcings, but to a lesser degree relative to T_{max} indices. A similar comparison can be made with regard to internal forcings.

4.5.2 Spatial variability of extremes over Australia

To assess spatial variability patterns, standard deviations (σ) of time series were calculated for each grid box between 1001 and 1850 for all forcings simulation (OGSV) and orbital only (O; Figure 4.13). Both simulations give rise to almost identical spatial patterns of year-to-year variability. By far, *coldest days* exhibits the highest year-to-year variability producing a standard deviation of 2.6°C in north western Australia. Relative year-to-year variability for this index follows a decreasing gradient to south eastern Australia ($\sigma = 0.8^\circ\text{C}$). *Hottest days* follows an increasing gradient from least year-to-year variability in the west ($\sigma = 0.8^\circ\text{C}$) to largest year-to-year variability in the east ($\sigma = 1.9^\circ\text{C}$). *Hottest nights* follows an increasing gradient from the least year-to-year variabil-

ity in the north ($\sigma = 0.6^\circ\text{C}$) to the most year-to-year variability in the south ($\sigma = 2.1^\circ\text{C}$). *Coldest nights*, is the one index not to exhibit any strong spatial patterns for year-to-year variability and has a standard deviation range of 0.5 to 1.7°C . Across all indices central Australia maintains moderate year-to-year variability.

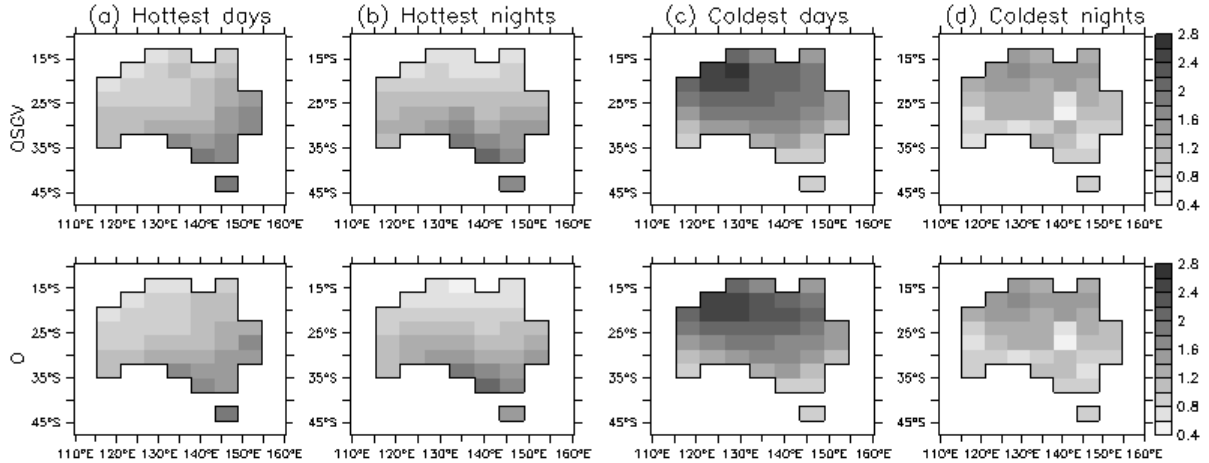


Figure 4.13: The standard deviations ($^\circ\text{C}$) of time series calculated at each grid point between 1001 and 1850 for forced simulations OGSV and O. the spatial distribution and magnitude remain almost identical under other forced simulations.

Whilst it is not shown, other forced simulations (OG, OGS and OGV) give rise to similar year-to-year variability. Thus, these spatial patterns are not influenced by external forcing and the result of unforced variability.

Summary of spatial variability

Coldest days are most variable in north east Australia; *hottest days* in south eastern Australia, and *hottest nights* in southern Australia. *Coldest nights* does not exhibit a strong pattern but generally has the largest variability in northern Australia. These spatial patterns persist regardless of external forcings (Figure 4.13).

4.6 Summary of results

1. Internal modes of variability influence all temperature extremes to varying degrees. *Coldest days* exhibits considerably larger interannual variability; also maintaining the strongest relationships with internal modes of variability, relative to other indices.
2. No statistically significant anomalies are associated with changes to solar irradiance. Large and abrupt cooling occurs subsequently to volcanic eruptions. The presence of solar forcing changes the influence volcanic eruptions have on temperature extremes.
3. Anthropogenic greenhouse gases dominate temperature extremes during the industrial period.
4. Each temperature index has its own pattern of spatial variability that persists irrespective of external forcings.
5. The magnitude exhibited by external forcings, greenhouse gases and internal climate drivers is not necessarily proportional to the signal witnessed in temperature extremes.

Chapter 5

Discussion

5.1 External Drivers of temperature extremes

Few studies to date have comprehensively assessed the influence of solar or volcanic forcings on temperature extremes. Here, I discuss these dynamical relationships in relation to the literature, suggest improved methodologies and highlight areas that would benefit from future research.

5.1.1 Volcanic eruptions

It is clear that the inclusion of volcanism in model simulations is required to reproduce certain the temperature anomalies that have occurred over the last millennium (compare simulation O, Figure 4.9 and simulation OGV, Figure 4.2b). The magnitude of the volcanic signal is greatest in *hottest nights* followed by *hottest days* and *coldest nights* (Figure 4.3). The magnitude of the signal evident in these three indices suggests a possible seasonal response to volcanic eruptions. Seasonal variations have been found in

NH assessments due to changes in circulation patterns but these relationships are strongly regional dependent (Shindell *et al.*, 2003; Shindell, 2004; Mann, 2007) and therefore may not be applicable for the SH or Australia. However others have found seasonal variations to lack significance (Crowley, 2000).

Few studies have assessed the seasonal influence of volcanic eruptions, particularly in the SH, and no such work has assessed the impact on day or night time temperature extremes. In this study, Australian cooling subsequent to volcanic eruptions is larger for T_{max} (summer) than T_{min} (winter) extremes. Within the model, dispersal of volcanic aerosols do not rely on circulation patterns because volcanic forcing is applied uniformly across the globe (Phipps *et al.*, 2012b). Whilst seasonal circulation patterns may still give rise to differences between T_{max} and T_{min} responses within the model, it may also be due to the internal climate dynamics driving individual indices. Within seasonal responses, nights were more influenced than days. The temporary cooling of one to four years subsequent to volcanic eruptions agrees with the results of other studies (e.g. Shindell, 2004).

Repetitive explosive volcanic eruptions appear to have an amplifying effect on temperature extremes (Section 4.2). It is not only the magnitude but also the frequency of volcanic eruptions that drive climate, and volcanoes that erupt in quick succession can have an amplifying effect (Miller *et al.*, 2012). In the absence of solar forcing, the eruption of 1258 exhibits a similar response to Tambora (Figure 4.2b) even though 1258 produced a larger radiative forcing (Figure 2.1). This may be due to several smaller eruptions preceding Tambora (Miller *et al.*, 2012), to self limiting effects of very large explosive eruptions (Pinto *et al.*, 1989) or to internal variability.

5.1.2 Solar Irradiance

Here, no significant changes to temperature extremes were found during periods of anomalous TSI (Section 4.2.3). The literature surrounding this issue is contentious as to whether the relationship between TSI and temperature is large (e.g. Shindell *et al.*, 2003; Servonnat *et al.*, 2010), small (e.g. Wagner & Zorita, 2005) or complex (e.g. Rind, 2002; Mann, 2007). Solar forcing mechanisms operate on a wide range of time scales and interact with many modes of internal variability that may amplify the forcing itself (Rind, 2002). For this reason, understanding the extent of TSI anomalies is difficult, and this is reflected in the literature where TSI anomalies are identified to be the driver of many varied mechanisms. I propose that TSI variability is a contributing forcing in combination with other external forcings and feedbacks within the climate system but in isolation does not have a detectable impact upon temperature extremes.

5.1.3 Dynamic duo volcanic and solar forcings

The results of this study agree with the well-established finding that volcanism and TSI anomalies are dominant drivers of climate over the pre-industrial component of the last millennium (e.g. Crowley, 2000; Bauer, 2003; Mann, 2007). Whilst numerous studies have focused on the NH, Phipps *et al.* (2012a) compare both hemispheres and find that the impact of solar and volcanic forcings is stronger in the SH.

Use of composites (e.g. Figure 4.7) may result in certain eruptions or TSI anomalies masking the signal of others. However, used in conjunction with assessments of individual volcanic simulations, composites are a useful tool. The influence of volcanic eruptions on all temperature extreme indices are temporally extended with the inclusion of solar forcing (Figure 4.7). The results of this study indicate volcanism plays a larger role,

agreeing with Wagner & Zorita (2005).

To more robustly identify relationships between TSI variability and volcanism on temperature extremes, it would be beneficial to construct composites of explosive eruptions during periods of high and low TSI anomalies. As the impact of explosive eruptions is short-lived, assessment of anomalous high and low TSI periods that coincide with periods of high and low volcanic activity would beneficially allow study of an extended time period.

5.1.4 Anthropogenic Forcing

Within the model, it is necessary to include anthropogenic GHG to successfully produce the changes in climate extremes observed over the industrial period. The model agrees with observed trends in finding that *coldest nights* exhibit the largest increasing trends, followed by *coldest days*, *hottest nights* and *hottest days*, over the second half of the twentieth century. As model evaluation was performed over the industrial period, it is not possible to say whether the model's tendency to over/underestimate the trend and magnitude of extreme indices represents deficiencies in the model's physics or in the forcings applied to the model. Extrapolating the model's tendency to over/underestimate trends to the entire twentieth century whilst considering simulation OG, suggests *hottest nights* is most influenced, followed by *hottest days*, *coldest days* and *coldest nights*.

This study finds extreme indices to respond differently to changes in GHG relative to other external forcings. There is a relationship between increasing concentrations of GHG and the amount of moisture in the atmosphere. Atmospheric moisture and cloudiness influence the planetary energy budget by similar mechanisms, and therefore act similarly as determinants of temperature. The signal from external forcings relative to internal

climate drivers (or vice versa) also indicates relative susceptibility of an extreme index to GHG.

The results of this study find *coldest nights* receives little influence from cloudiness or external forcings and accordingly receive little influence from anthropogenic GHG. *Hottest days* are not influenced by cloudiness but its variability appears to be driven by external forcings. Accordingly *hottest days* are reasonably influenced by changes in anthropogenic GHG. *Hottest nights* and *coldest days* are found to be cloud influenced indices. *Coldest days* exhibits a strong signal from anthropogenic GHG relative to its response to other external forcings and this is likely due to the similar physical mechanisms that relate GHG and cloudiness to surface temperature. *Hottest nights* is most impacted upon by anthropogenic GHG, followed by *hottest days*, *coldest days* and *coldest nights*. Thus the physical mechanisms of natural variability that drive temperature extremes can be extrapolated to understand why certain indices are more or less influenced by changes to external forcings.

The influence of increasing GHG on internal variability was not assessed in this study as the analysis of internal variability was kept to the pre-industrial period only. However, SLP, cloudiness and SST will all change in a warming world. Moisture content will increase, SST will rise, and storm tracks in the SH will shift poleward (Bengtsson *et al.*, 2006). These changes are relevant for all indices assessed here. Note that this analysis looks at the influence of greenhouse gases in isolation from other forcings. The model does not consider anthropogenically induced changes to tropospheric aerosols, stratospheric ozone, vegetation or land cover which can also influence temperature extremes (Avila *et al.*, 2012).

5.2 Variability of Australian temperature extremes

Whilst this study did not focus extensively on varying modes of natural variability, it did assess some of the most significant climate variables (SST, SLP, cloudiness) that may drive temperature extremes. Thus, findings from this present study indicate the degree to which natural variability drives temperature extremes in Australia. Here I discuss the variability of Australian temperature extremes over the millennium in light of these internal drivers.

Internal variability is thought to be influenced by external forcings to at least some extent, though this relationship is somewhat unclear (Rind, 2002; Mann & Cane, 2005; D'Arrigo, 2005; Phipps & Brown, 2010). It is likely that modes of internal variability and extensive feedback loops determine down to smaller and smaller scales the degree to which external forcings drive temperature extremes. The assessments of internal variability here, use Australian averages. Therefore, certain climatic regions within Australia may mask the signal of others (e.g. arid vs. temperate zone). In the future, it would be of particular interest to assess the spatial distribution of these relationships. Furthermore, it is likely that the relative influence of internal modes of variability on temperature indices is specific to Australia. Previous works have identified strong relationships between ENSO and Australian temperature extremes (Kenyon & Hegerl, 2008; Alexander *et al.*, 2009; Arblaster & Alexander, 2012). In comparison the ENSO relationships identified in this study are relatively weak. This study correlated temperature extremes against seasonal SST for each year during the pre-industrial period, irrespective of whether ENSO events occurred and their strength. The prevalence of an ENSO signal may indeed suggest a strong relationship with temperature extremes.

Hottest days displays a high correlation with ENSO patterns; particularly the Niño 3 and Niño 4 regions. ENSO is known to have a strong influence on Australian climate and

temperature variability. *Hottest days* is negatively correlated with cloudiness but not to the same degree as *coldest days*. This is expected as increasing cloudiness proportionally increases the extremity of *coldest days*. Many variables associated with cloudiness; for example, density, thickness, height provide scope for large temporal and spatial variability of cloudiness and therefore, highly variable impacts. This study has found a strong relationship between the variability of cloudiness and *coldest days*, which is characterised by much larger interannual variability relative to the other indices. *Hottest days* will generally occur on days with no clouds, therefore the variability of this index is unlikely to be related.

Cloudiness dampens day time temperatures (*coldest days*) more than it warms night time temperatures (emphhottest nights; Dai *et al.*, 1999). Dai *et al.* (1999) attributed decreases in diurnal temperature range to increasing daytime cloudiness over the latter half of the twentieth century. Throughout this study *coldest days* has stood out from the other indices. It has high interannual variability and exhibits a weak response relative to other indices when forced with external drivers. Whilst the model over-estimated the interannual variability of *coldest days*, observations also find it to be the most variable index relative to the other indices. The signal from internal climate drivers is strong relative to external forcings for *coldest days*. This relationship therefore limits the signal of all external forcings relative to other indices.

Coldest days has strong correlations with SLP, SST and cloudiness. *Coldest days* is the only temperature index to exhibit strong correlations with all three variables, and is thus largely influenced by internal climate drivers. Correlations with IOD and cloudiness account for half the interannual variability exhibited by *coldest days*. Strong positive (northeast Indian Ocean) and negative (southeast Indian Ocean) correlations between *coldest days* and SLP may be related to atmospheric blocking (Matsueda, 2011; Bengtsson *et al.*, 2006) and/or the Australian Monsoon (Risbey *et al.*, 2009).

Many modes of internal variability act on smaller timescales than external forcings. Modes of internal variability respond to external drivers and therefore, exhibit indirect influences on the climate that may be even larger than the external forcings themselves.

Whilst the model overestimates the intensity of *hottest nights*, it only slightly underestimates its trend and interannual variability relative to observations over 1957 to 2000. It does not have a strong or clear relationship with ENSO, PDO or IOD, however it does have a positive correlation with cloudiness. While *hottest nights* does not exhibit a correlation with ENSO through SST, the pattern of correlation with SLP indicates a relationship with an easterly wind across Australia. Lack of a strong ENSO signal may be due to varying regional responses within Australia or deficiencies in the simulated ENSO.

It is likely that night time convection has a strong influence on coastal temperatures. However, assessment of Australian averages may mask the influence of night time convection on temperature extremes. Time constraints did not allow assessment of spatially distributed correlations, which would aid understanding of regional processes within Australia; particularly for *hottest nights* but for all extreme temperature indices assessed here.

The net effect of cloudiness on maximum night time temperatures is generally small (Kenyon & Hegerl, 2008), agreeing with the findings of this study. Both cloudiness and GHG influence temperature extremes in similar ways by altering the surface radiation balance. *Hottest nights* is influenced to a large degree by GHG concentrations but not cloudiness. This may indicate that cloudiness is not nearly as variable during the night as it is during the day. It appears that the variability of T_{max} indices are more broadly influenced by external forcings and less driven by internal variability relative to other indices. Throughout this study external forcings have been consistently identified to

drive *hottest nights*.

Coldest nights do not exhibit strong signals from either external or internal drivers. It has slightly higher interannual variability and is less influenced by external forcings than T_{max} indices. *Coldest nights* receives more influence from internal variability than T_{max} indices, but less than *coldest days*. One reason for this may be the lack of correlation between *coldest nights* and cloudiness, which seems to be a large driver of variability for *coldest days*. However, this does not explain the weak signal exhibited by *coldest nights* when forced with changes in external forcings.

The spatial variability exhibited by each extreme index persists regardless of external forcing. Surprisingly, there is no consistent correlation between areas of high or low variability being impacted upon first, last, most or least when forced with anomalous external drivers.

5.3 Other limitations of this study

It should be emphasised that this study is based on a single climate model and so results from this study may be biased by deficiencies in the model physics or omitted forcings. Reconstructions used to force the model are derived from proxies which are accompanied by uncertainties (Mann *et al.*, 2008). Only four temperature indices were assessed and these indices looked at the most extreme hottest and coldest days and nights of the year. Therefore, they may not be accurate representations of seasonal or annual temperatures.

Chapter 6

Conclusions and future work

6.1 Conclusions

Before understanding how entities act together when combined, it is necessary to first understand their individual behaviour. This study has attempted to do this from two angles. Firstly, it has attempted to understand the behaviour of external forcings (solar, volcanic and anthropogenic) and secondly it has attempted to understand the behaviours of four different indices of extreme temperature. This understanding can aid projections of how the climate may be influenced in the future and what impacts can be expected from anomalous external forcings.

Overall, the degree to which external drivers influence temperature extremes is not necessarily proportional to the strength of forcing. Thus, the relationship is not simple or direct and is also dependent on internal variability. The reason as to why respective mechanisms influence only particular indices is unique to each index and is dependent on many feedback relationships. Thus, the degree to which temperature extremes are

influenced by external forcings is dependent on the variability and strength of both internal and external forcings and also feedback loops which include the temperature extreme indices themselves.

1. Internal modes of variability influence all temperature extremes to varying degrees. *Coldest days* exhibits the largest interannual variability of all forcings and this is driven by internal variability. The main reason for this is the large influence of cloudiness on this index.
2. No statistically significant anomalies are associated with changes to solar irradiance. Large and abrupt cooling occurs subsequently to volcanic eruptions. Solar minima enhance T_{max} cooling and solar maxima dampen anomalous T_{min} cooling in combination with volcanic eruptions.
3. Over the twentieth century, GHG concentrations became an increasingly dominant driver of temperature extremes.
4. T_{max} indices are more influenced by changes to external forcings relative to T_{min} indices.

6.2 Future work

This study has highlighted important relationships between temperature extremes, external forcings and modes of internal variability. The conclusions of this study highlight key relationships that would benefit from further research.

The study has focused on the relationship between external forcings and temperature extremes, but it has become apparent that this relationship can only be explained in

collaboration with internal variability. Therefore, understanding the relationship between external forcing and internal modes of variability is a significant stepping stone on the path to robustly understanding the behaviour of temperature extremes. Formal detection and attribution studies provide a valuable tool. Assessment of ensembles rather than individual simulations would better capture the influence of natural variability. Of course there is potential to expand analysis to other regions and also further back in time. Assessment of other global and regional climate models, in collaboration with proxies would aid analysis of natural variability and climate change over past millennia. The quality of proxy records should denote appropriate time periods for assessment.

The ability to apply knowledge comes not only from understanding which mechanisms drive indices but how they drive them. This knowledge will allow projection of future changes and the extrapolation of identified physical relationships to other phenomena.

Analysis of a more extensive set of indices, including precipitation would increase understanding of the climate system. Assessment of apparent temperature indices would be of benefit to policy makers and those interested in adapting to and mitigating current and future climate change.

Bibliography

- Adger, W.N., Huq, S., Brown, K., Conway, D., & Hulme, M. 2003. Adaptation to climate change in the developing world. *Progress in development studies*, **3**(3), 179–195.
- Alexander, L, Zhang, X, Peterson, T C, Caesar, J, Gleason, B, Klein Tank, A M G, & et al. 2006. Global observed changes in daily climate extremes of temperature and precipitation. *Journal of Geophysical Research*, **111**, D05109.
- Alexander, L V, & Arblaster, J M. 2009. Assessing trends in observed and modelled climate extremes over Australia in relation to future projections. *International Journal of Climatology*, **29**, 417–435.
- Alexander, Lisa V., Uotila, Petteri, & Nicholls, Neville. 2009. Influence of sea surface temperature variability on global temperature and precipitation extremes. *Journal of Geophysical Research*, **114**(D18).
- Alexander, LV, Hope, Pandora, & Collins, Dean. 2007. Trends in Australia's climate means and extremes: a global context. *Australian Meteorological Magazine*, **56**(1), 1–18.
- Allen, Mr, Stott, Pa, Mitchell, Jf, Schnur, R, & Delworth, Tl. 2000. Quantifying the uncertainty in forecasts of anthropogenic climate change. *Nature*, **407**(6804), 617–20.
- Arblaster, J.M., & Alexander, L.V. 2012. The impact of the El Niño Southern Oscillation on maximum temperature extremes. *Geophysical Research Letters*, **39**, L20702.
- Avila, F. B., Pitman, a. J., Donat, M. G., Alexander, L. V., & Abramowitz, G. 2012. Climate model simulated changes in temperature extremes due to land cover change. *Journal of Geophysical Research*, **117**, D04108.
- Bauer, Eva. 2003. Assessing climate forcings of the Earth system for the past millennium. *Geophysical Research Letters*, **30**(6), 1–4.
- Bengtsson, L, Hodges, KI, & Roeckner, E. 2006. Storm tracks and climate change. *Journal of Climate*, **19**, 3518–3543.
- Bengtsson, Lennart, Hagemann, Stefan, & Hodges, Kevin I. 2004. Can climate trends be calculated from reanalysis data? *Journal of Geophysical Research*, **109**(D11), 1–8.

- Berger, AL. 1978. Long-term variations of daily insolation and Quaternary climatic changes. *Journal of the Atmospheric Sciences*, **35**, 2362—2367.
- Bradley, R.S., Briffa, K.R., Cole, J., Hughes, M.K., & Osborn, T.J. 2003. The climate of the last millennium. *Paleoclimate, Global Change and the Future*, 105–141.
- Brands, S., Gutiérrez, J. M., Herrera, S., & Cofiño, a. S. 2012. On the Use of Reanalysis Data for Downscaling. *Journal of Climate*, **25**(7), 2517–2526.
- Briffa, Keith R., & Osborn, Timothy J. 2002. Blowing hot and cold. *Science*, **295**, 2227–8.
- Caesar, John, Alexander, L, & Vose, R. 2006. Large-scale changes in observed daily maximum and minimum temperatures: Creation and analysis of a new gridded data set. *Journal of Geophysical Research*, **111**, D05101.
- Collier, MA, Jeffrey, SJ, Rotstayn, LD, Wong, KK, Dravitzki, SM, Moseneder, C., Hamalainen, C., Syktus, JI, Suppiah, R., Antony, J., *et al.* 2011. The CSIRO-Mk3. 6.0 Atmosphere-Ocean GCM: participation in CMIP5 and data publication. *In: International Congress on Modelling and Simulation—MODSIM 2011*.
- Collins, DA, & Della-Marta, PM. 2000. Trends in annual frequencies of extreme temperature events in Australia. *Australian Meteorological Magazine*, **49**(4), 277–292.
- Crowley, T. J. 2000. Causes of Climate Change Over the Past 1000 Years. *Science*, **289**, 270–277.
- Crowley, T J, Zielinski, G, Vinther, B, Udisti, R, Kreutz, K, Cole-Dai, J, & Castellano, E. 2008. Volcanism and the Little Ice Age. *PAGES News*, **16**, 22–23.
- Dai, A, Trenberth, KE, & Karl, TR. 1999. Effects of clouds, soil moisture, precipitation, and water vapor on diurnal temperature range. *Journal of Climate*, **12**, 2451–2473.
- D'Arrigo, Rosanne. 2005. On the variability of ENSO over the past six centuries. *Geophysical Research Letters*, **32**(3), 2–5.
- Diaz, H.F., Trigo, R., Hughes, M.K., Mann, M.E., Xoplaki, E., & Barriopedro, D. 2011. Spatial and temporal characteristics of climate in Medieval Times revisited. *Bulletin of the American Meteorological Society*, **92**(11), 1487.
- Donat, Markus, Alexander, LV, Yang, H, Durre, I, Vose³, R, Dunn, RJH, Willett, KM, Aguilar, E, Brunet, M., Caesar, J, Hewitson, B, Jack, C, Tank, AMG Klein, Kruger, AC, Marengo, J, Peterson, TC, Renom, M, Rojas, C Oria, Rusticucci, M, Salinger, J, Sekele, SS, Srivastava, AK, Trewin, B, Villarroel, C, Vincent, LA, Zhai, P, Zhang, X, & Kitching, S 8. 2012a. Updated analyses of temperature and precipitation extreme indices since the beginning of the twentieth century: The HadEX2 dataset. *Journal of Geophysical Research - submitted*.
- Donat, Markus G., & Alexander, Lisa V. 2012. The shifting probability distribution of global daytime and night-time temperatures. *Geophysical Research Letters*, **39**, L14707.

- Donat, Markus G, Alexander, Lisa V, Vose, Russ, & Donat, Markus. 2012b. Global land-based datasets for monitoring climatic extremes. *Bulletin of the American Meteorological Society* - submitted.
- Durre, Imke, Menne, Matthew J., Gleason, Byron E., Houston, Tamara G., & Vose, Russell S. 2010. Comprehensive Automated Quality Assurance of Daily Surface Observations. *Journal of Applied Meteorology and Climatology*, **49**(8), 1615–1633.
- Easterling, D.R., Meehl, G.A., Parmesan, C., Changnon, S.A., Karl, T.R., & Mearns, L.O. 2000. Climate extremes: observations, modeling, and impacts. *Science*, **289**(5487), 2068–2074.
- Fernández-Donado, L., González-Rouco, J. F., Raible, C. C., Ammann, C. M., Barriopedro, D., García-Bustamante, E., Jungclaus, J. H., Lorenz, S. J., Luterbacher, J., Phipps, S. J., Servonnat, J., Swingedouw, D., Tett, S. F. B., Wagner, S., Yiou, P., & Zorita, E. 2012. Temperature response to external forcing in simulations and reconstructions of the last millennium. *Climate of the Past Discussions*, **8**(4), 4003–4073.
- Foukal, P., Fröhlich, C., Spruit, H., & Wigley, TML. 2006. Variations in solar luminosity and their effect on the Earth’s climate. *Nature*, **443**(7108), 161–166.
- Frich, P, Alexander, L V, Gleason, B, Haylock, M, Tank, A M G Klein, & Peterson, T. 2002. Observed coherent changes in climatic extremes during the second half of the twentieth century. *Climate Research*, **19**, 193–212.
- Friedel, MH, Foran, BD, & Stafford Smith, DM. 1990. Where the creeks run dry or ten feet high: pastoral management in arid Australia.[Symposium paper]. *In: Proceedings of the Ecological Society of Australia*, vol. 16. Ecological Society of Australia.
- Gordon, H.B., Rotstayn, LD, McGregor, JL, Dix, MR, Kowalczyk, EA, OFarrell, SP, Waterman, LJ, Hirst, AC, Wilson, SG, Collier, MA, *et al.* 2002. *The CSIRO Mk3 climate system model*. Vol. 130. CSIRO Atmospheric Research.
- Haylock, Malcolm, & Nicholls, Neville. 2000. Trends in extreme rainfall indices for an updated high quality data set for Australia, 1910-1998. *International Journal of Climatology*, **20**(13), 1533–1541.
- Hegerl, Gabriele C., Crowley, Thomas J., Allen, Myles, Hyde, William T., Pollack, Henry N., Smerdon, Jason, & Zorita, Eduardo. 2007. Detection of Human Influence on a New, Validated 1500-Year Temperature Reconstruction. *Journal of Climate*, **20**(4), 650–666.
- Hendon, Harry H. 2003. Indonesian Rainfall Variability: Impacts of ENSO and Local AirSea Interaction. *Journal of Climate*, **16**(11), 1775–1790.
- Hendon, Harry H., Thompson, David W. J., & Wheeler, Matthew C. 2007. Australian Rainfall and Surface Temperature Variations Associated with the Southern Hemisphere Annular Mode. *Journal of Climate*, **20**(11), 2452–2467.

- Hughes, MK, & Diaz, HF. 1994. Was there a 'medieval warm period', and if so, where and when? *Climatic Change*, **26**, 109–142.
- Jones, DA, & Trewin, BC. 2000. On the relationships between the El Niño Southern Oscillation and Australian land surface temperature. *International Journal of Climatology*, **20**, 697–719.
- Jones, David A, & Wang, William. 2009. High-quality spatial climate data-sets for Australia. *Australian Meteorological and Oceanographic Journal*, **58**, 233–248.
- Jones, P D, & Mann, M E. 2004. Climate over past millennia. *Review of Geophysics*, **42**, RG2002.
- Jones, P D, Osborn, T J, & Briffa, K R. 2001. The evolution of climate over the last millennium. *Science*, **292**(5517), 662–7.
- Jones, PD, Briffa, KR, & Osborn, TJ. 2009. High-resolution palaeoclimatology of the last millennium: a review of current status and future prospects. *The Holocene*, **19**(1), 3–49.
- Karl, T R, & Easterling, D R. 1999. Climate extremes: selected review and future research directions. *Climate Change*, **42**, 309–325.
- Kenyon, Jesse, & Hegerl, Gabriele C. 2008. Influence of Modes of Climate Variability on Global Temperature Extremes. *Journal of Climate*, **21**(15), 3872–3889.
- Kharin, V V, Zwiers, F W, Zhang, X, & Hegerl, G C. 2007. Changes in Temperature and Precipitation Extremes in the IPCC Ensemble of Global Coupled Model Simulations. *Journal of Climate*, **20**, 1419–1444.
- Kiktev, D, Caesar, J, Alexander, L V, Shiogama, H, & Collier, M. 2007. Comparison of observed and multimodeled trends in annual extremes of temperature and precipitation. *Geophysical Research Letters*, **34**, 2–6.
- Lamb, H.H. 1965. The early medieval warm epoch and its sequel. *Palaeogeography, Palaeoclimatology, Palaeoecology*, **1**, 13–37.
- Li, Jinbao, Xie, Shang-Ping, Cook, Edward R., Huang, Gang, D'Arrigo, Rosanne, Liu, Fei, Ma, Jian, & Zheng, Xiao-Tong. 2011. Interdecadal modulation of El Niño amplitude during the past millennium. *Nature Climate Change*, **1**(2), 114–118.
- Luterbacher, Jürg, Dietrich, Daniel, Xoplaki, Elena, Grosjean, Martin, & Wanner, Heinz. 2004. European seasonal and annual temperature variability, trends, and extremes since 1500. *Science*, **303**(5663), 1499–503.
- MacFarling Meure, C, Etheridge, D, Trudinger, C, Steele, P, Langenfelds, R, van Ommen, T, Smith, A, & Elkins, J. 2006. Law Dome CO₂, CH₄ and N₂O ice core records extended to 2000 years BP. *Geophysical Research Letters*, **33**, 1–4.

- Mann, ME, & Cane, MA. 2005. Volcanic and solar forcing of the tropical Pacific over the past 1000 years. *Journal of Climate*, **18**, 447–456.
- Mann, Michael E. 2007. Climate Over the Past Two Millennia. *Annual Review of Earth and Planetary Sciences*, **35**, 111–136.
- Mann, Michael E, Zhang, Zhihua, Hughes, Malcolm K, Bradley, Raymond S, Miller, Sonya K, Rutherford, Scott, & Ni, Fenbiao. 2008. Proxy-based reconstructions of hemispheric and global surface temperature variations over the past two millennia. *Proceedings of the National Academy of Sciences of the United States of America*, **105**(36), 13252–7.
- Mann, Michael E, Zhang, Zhihua, Rutherford, Scott, Bradley, Raymond S, Hughes, Malcolm K, Shindell, Drew, Ammann, Caspar, Faluvegi, Greg, & Ni, Fenbiao. 2009. Global signatures and dynamical origins of the Little Ice Age and Medieval Climate Anomaly. *Science*, **326**(5957), 1256–60.
- Matsueda, M. 2011. Predictability of Euro-Russian blocking in summer of 2010. *Geophysical Research Letters*, **38**(6), L06801.
- Matthes, F.E. 1939. Report of the Committee on Glaciers. *Transactions of the American Geophysical Union*, **20**, 518–523.
- McPhaden, M.J., Zebiak, S.E., & Glantz, M.H. 2006. ENSO as an integrating concept in earth science. *Science*, **314**(5806), 1740–1745.
- Meehl, Gerald a., Covey, Curt, Taylor, Karl E., Delworth, Thomas, Stouffer, Ronald J., Latif, Mojib, McAvaney, Bryant, & Mitchell, John F. B. 2007. THE WCRP CMIP3 Multimodel Dataset: A New Era in Climate Change Research. *Bulletin of the American Meteorological Society*, **88**(9), 1383–1394.
- Miller, G.H., Geirsdóttir, Á., Zhong, Y., Larsen, D.J., Otto-Bliesner, B.L., Holland, M.M., Bailey, D.A., Refsnider, K.A., Lehman, S.J., Southon, J.R., *et al.* 2012. Abrupt onset of the Little Ice Age triggered by volcanism and sustained by sea-ice/ocean feedbacks. *Geophysical Research Letters*, **39**(2), L02708.
- Min, Seung-Ki, Zhang, Xuebin, Zwiers, Francis W, & Hegerl, Gabriele C. 2011. Human contribution to more-intense precipitation extremes. *Nature*, **470**(7334), 378–81.
- Nicholls, N., & Alexander, L. 2007. Has the climate become more variable or extreme? Progress 1992-2006. *Progress in Physical Geography*, **31**(1), 77–87.
- Osborn, T.J., & Briffa, K.R. 2006. The spatial extent of 20th-century warmth in the context of the past 1200 years. *Science*, **311**(5762), 841–844.
- Perkins, S E, Pitman, A J, Holbrook, N J, & McAneney, J. 2007. Evaluation of the AR4 Climate Models Simulated Daily Maximum Temperature, Minimum Temperature, and Precipitation over Australia Using Probability Density Functions. *Journal of Climate*, **20**, 4356–4376.

- Phipps, S J, Rotstayn, L D, Gordon, H B, Roberts, J L, Hirst, A C, & Budd, W F. 2011. The CSIRO Mk3L climate system model version 1.0 Part 1: Description and evaluation. *Geoscientific Model Development*, **4**, 483–509.
- Phipps, S. J., McGregor, H. V., Gergis, J., Gallant, A. J. E., Neukom, R., Stevenson, S., Ackerley, D., Brown, J. R., Fischer, M. J., & van Ommen, T. D. 2012a. Paleoclimate data-model comparison and the role of climate forcings over the past 1500 years. *Journal of Climate*, *in revision*.
- Phipps, S J, Rotstayn, L D, Gordon, H B, Roberts, J L, Hirst, A C, & Budd, W F. 2012b. The CSIRO Mk3L climate system model version 1.0 Part 2: Response to external forcings. *Geoscientific Model Development*, **5**, 649–682.
- Phipps, Steven J, & Brown, Jaclyn N. 2010. Understanding ENSO dynamics through the exploration of past climates. *IOP Conference Series: Earth and Environmental Science*, **9**, 012010.
- Pinto, J.P., Turco, R.P., & Toon, O.B. 1989. Self-limiting physical and chemical effects in volcanic eruption clouds. *Journal of Geophysical Research*, **94**(D8), 11165–11.
- Plummer, N., Salinger, MJ, & Nicholls, N. 1999. Changes in climate extremes over the Australian region and New Zealand during the twentieth century. *Climatic Change*, **42**(1), 183–202.
- Rind, D. 2002. The Sun’s role in climate variations. *Science (New York, N.Y.)*, **296**(5568), 673–7.
- Risbey, James S., Pook, Michael J., McIntosh, Peter C., Wheeler, Matthew C., & Hendon, Harry H. 2009. On the Remote Drivers of Rainfall Variability in Australia. *Monthly Weather Review*, **137**(10), 3233–3253.
- Robock, A. 2000. Volcanic eruptions and climate. *REVIEWS OF GEOPHYSICS-RICHMOND VIRGINIA THEN WASHINGTON-*, **38**(2), 191–220.
- Saji, N H, Goswami, B N, Vinayachandran, P N, & Yamagata, T. 1999. A dipole mode in the tropical Indian Ocean. *Nature*, **401**(6751), 360–3.
- Sanotoso, A., Cai, W., England, M. H., & Phipps, S.J. 2011. The Role of the Indonesian Throughflow on ENSO Dynamics in a Coupled Climate Model. *Journal of Climate*, **24**, 585–601.
- Scaife, Adam a., Folland, Chris K., Alexander, Lisa V., Moberg, Anders, & Knight, Jeff R. 2008. European Climate Extremes and the North Atlantic Oscillation. *Journal of Climate*, **21**(1), 72–83.
- Schmidt, G. a., Jungclaus, J. H., Ammann, C. M., Bard, E., Braconnot, P., Crowley, T. J., Delaygue, G., Joos, F., Krivova, N. a., Muscheler, R., Otto-Bliesner, B. L., Pongratz, J., Shindell, D. T., Solanki, S. K., Steinhilber, F., & Vieira, L. E. a. 2012. Climate forcing reconstructions for use in PMIP simulations of the Last Millennium (v1.1). *Geoscientific Model Development*, **5**, 185–191.

- Seneviratne, S.I., Nicholls, N., Easterling, D., Goodess, C.M., Kanae, S., and Y. Luo, J. Kossin, Marengo, J., Innes, K., Rahimi, M., Reichstein, M., Sorteberg, A., Vera, C., & Zhang., X. 2012. Changes in climate extremes and their impacts on the natural physical environment. *Managing the Risks of Extreme Events and Disasters to Advance Climate Change Adaptation*.
- Servonnat, J., Yiou, P., Khodri, M., Swingedouw, D., & Denvil, S. 2010. Influence of solar variability, CO₂ and orbital forcing between 1000 and 1850 AD in the IPSLCM4 model. *Climate of the Past*, **6**(4), 445–460.
- Shindell, Drew T. 2004. Dynamic winter climate response to large tropical volcanic eruptions since 1600. *Journal of Geophysical Research*, **109**(D5), 1–12.
- Shindell, Drew T., Schmidt, Gavin A., Miller, Ron L., & Mann, Michael E. 2003. Volcanic and Solar Forcing of Climate Change during the Preindustrial Era. *Journal of Climate*, **16**, 4094–4107.
- Sillmann, J, Kharin, V.V., Zhang, X., & Zwiers, F.W. 2012. Climate extreme indices in the CMIP5 multi-model ensemble. Part 1: Model evaluation in the present climate. *Journal of Geophysical Research - submitted*.
- Simmons, a. J. 2004. Comparison of trends and low-frequency variability in CRU, ERA-40, and NCEP/NCAR analyses of surface air temperature. *Journal of Geophysical Research*, **109**(D24), 1–18.
- Smith, Ian. 2004. An assessment of recent trends in Australian rainfall. *Australian Meteorological magazine*, **53**, 163–173.
- Smith, Joel B, Schneider, Stephen H, Oppenheimer, Michael, Yohe, Gary W, Hare, William, Mastrandrea, Michael D, Patwardhan, Anand, Burton, Ian, Corfee-Morlot, Jan, Magadza, Chris H D, Füssel, Hans-Martin, Pittock, a Barrie, Rahman, Atiq, Suarez, Avelino, & van Ypersele, Jean-Pascal. 2009. Assessing dangerous climate change through an update of the Intergovernmental Panel on Climate Change (IPCC) "reasons for concern". *Proceedings of the National Academy of Sciences of the United States of America*, **106**(11), 4133–7.
- Solomon, S., and M. Manning, D. Qin, Chen, Z., Marquis, M., Averyt, K.B., Tignor, M., & Miller, H.L. 2007a. *Climate Change 2007 - The Physical Science Basis: Working Group I Contribution to the Fourth Assessment Report of the IPCC*. Climate Change 2007. Cambridge University Press.
- Solomon, S, Qin, D., Manning, M., Chen, Z., Marquis, M., Averyt, K.B., Tignor, M., & (eds.), H.L. Miller. 2007b. *Contribution of Working Group I to the Fourth Assessment Report of the Intergovernmental Panel on Climate Change, 2007*. Cambridge, United Kingdom and New York, NY, USA.: Cambridge University Press.
- Steinhilber, F, Beer, J, & Fröhlich, C. 2009. Total solar irradiance during the Holocene. *Geophysical Research Letters*, **36**, L19704.

- Steinhilber, F., Abreu, J.A., Beer, J., Brunner, I., Christl, M., Fischer, H., Heikkilä, U., Kubik, P.W., Mann, M., McCracken, K.G., *et al.* 2012. 9,400 years of cosmic radiation and solar activity from ice cores and tree rings. *Proceedings of the National Academy of Sciences*, **109**(16), 5967–5971.
- Stott, Peter a, & Kettleborough, J a. 2002. Origins and estimates of uncertainty in predictions of twenty-first century temperature rise. *Nature*, **416**(6882), 723–6.
- Tebaldi, Claudia, Hayhoe, Katharinec, Arblaster, Julie M., & Meehl, Gerald a. 2006. Going to the Extremes. *Climatic Change*, **79**(3-4), 185–211.
- Tompkins, E.L., & Adger, W.N. 2004. Does adaptive management of natural resources enhance resilience to climate change? *Ecology and society*, **9**(2), 10.
- Trenberth, KE. 1997. The definition of el nino. *Bulletin of the American Meteorological Society*, 2771–2777.
- Trewin, B.C. 2001 (14-18 January). The development of a high-quality daily temperature data set for Australia. *Pages 279–84 of: Eleventh Symposium on Meteorological Observations and Instrumentation.*
- Vogel, Martha-Marie. 2012. *Uncertainties in Estimating Trends in Australia’s Coldest, Warmest and Wettest Extremes.* Ph.D. thesis, Climate Change Research Centre, University of New South Wales.
- Wagner, Sebastian, & Zorita, Eduardo. 2005. The influence of volcanic, solar and CO2 forcing on the temperatures in the Dalton Minimum (1790/1830): a model study. *Climate Dynamics*, **25**(2-3), 205–218.
- Wang, Guomin, & Hendon, Harry H. 2007. Sensitivity of Australian Rainfall to InterEl Niño Variations. *Journal of Climate*, **20**(16), 4211–4226.
- Wittenberg, Andrew T. 2009. Are historical records sufficient to constrain ENSO simulations? *Geophysical Research Letters*, **36**(12), 1–5.
- Zhang, X, Alexander, L V, Hegerl, G C, P, Tank Klein, A, Peterson, T C, B, & Zwiers. 2011. Indices for monitoring changes in extremes based on daily temperature and precipitation data. *Wiley Interdisciplinary Reviews: Climate Change*, **2**, 851–870.
- Zorita, E. 2005. Natural and anthropogenic modes of surface temperature variations in the last thousand years. *Geophysical Research Letters*, **32**(8), 2–5.